Disease Models & Mechanisms 6, 661-678 (2013) doi:10.1242/dmm.010066

In *Drosophila*, RhoGEF2 cooperates with activated Ras in tumorigenesis through a pathway involving Rho1–Rok–Myosin-II and JNK signalling

Peytee Khoo[1,2], Kirsten Allan[1], Lee Willoughby[1], Anthony M. Brumby[1,2] and Helena E. Richardson[1,2,3,4,*]

SUMMARY

The *Ras* oncogene contributes to ~30% of human cancers, but alone is not sufficient for tumorigenesis. In a *Drosophila* screen for oncogenes that cooperate with an activated allele of *Ras* (*Ras*^{ACT}) to promote tissue overgrowth and invasion, we identified the GTP exchange factor *RhoGEF2*, an activator of Rho-family signalling. Here, we show that RhoGEF2 also cooperates with an activated allele of a downstream effector of Ras, *Raf* (*Raf*^{GOF}). We dissect the downstream pathways through which RhoGEF2 cooperates with Ras^{ACT} (and Raf^{GOF}), and show that RhoGEF2 requires Rho1, but not Rac, for tumorigenesis. Furthermore, of the Rho1 effectors, we show that RhoGEF2 + Ras (Raf)-mediated tumorigenesis requires the Rho kinase (Rok)–Myosin-II pathway, but not Diaphanous, Lim kinase or protein kinase N. The Rho1–Rok–Myosin-II pathway leads to the activation of Jun kinase (JNK), in cooperation with Ras^{ACT}. Moreover, we show that activation of Rok or Myosin II, using constitutively active transgenes, is sufficient for cooperative tumorigenesis with Ras^{ACT}, and together with Ras^{ACT} leads to strong activation of JNK. Our results show that Rok–Myosin-II activity is necessary and sufficient for Ras-mediated tumorigenesis. Our observation that activation of Myosin II, which regulates Filamentous actin (F-actin) contractility without affecting F-actin levels, cooperates with Ras^{ACT} to promote JNK activation and tumorigenesis, suggests that increased cell contractility is a key factor in tumorigenesis. Furthermore, we show that signalling via the Tumour necrosis factor (TNF; also known as Egr)-ligand–JNK pathway is most likely the predominant pathway that activates JNK upon Rok activation. Overall, our analysis highlights the need for further analysis of the Rok–Myosin-II pathway in cooperation with Ras in human cancers.

INTRODUCTION

Cancer is a multi-step process involving the acquisition of genetic alterations that deregulate growth and apoptosis pathways, propelling normal cells into a malignant state (Vogelstein and Kinzler, 1993). The following changes in cell physiology arise from such genetic mutations and contribute to malignancy: self-sufficiency in growth signals, insensitivity to anti-growth signals, evasion of apoptosis, sustained angiogenesis, limitless replicative potential, tissue invasion and metastasis (Hanahan and Weinberg, 2000; Hanahan and Weinberg, 2011). Moreover, interactions between the developing tumour and surrounding cells can impact upon tumorigenesis.

Drosophila is an ideal model organism for studying cooperative tumorigenesis, owing to its sophisticated genetics, lower redundancy and fast generation time (Brumby and Richardson, 2005). For example, clonal analysis allows the generation of marked mutant clones with a number of genetic mutations within a wild-type context, enabling the examination of tumour development and the interaction of the tumour with the surrounding wild-type cells. In a two-hit model of tumorigenesis in *Drosophila*, cooperation was observed between a mutation in the apico-basal cell polarity regulator Scrib, combined with expression of an activated allele of *Ras* (*Ras*^{ACT}) in the developing eye-antennal tissue [eye-antennal discs (EADs)] (Brumby and Richardson, 2003). Although loss of *scrib* function (*scrib*^{1}) in clones on its own resulted in hyper-proliferation and altered cell morphology, mutant clones did not over-grow because they were removed by Jun kinase (JNK; also known as Bsk in *Drosophila*)-mediated apoptosis (Brumby and Richardson, 2003). Expression of *Ras*^{ACT} alone in clones in the developing EAD resulted in hyperplasia and ectopic differentiation. In contrast, *Ras*^{ACT} expression in *scrib* mutant EAD clones resulted in massive clonal tissue overgrowth due to increased proliferation, increased survival and loss of differentiation, and was associated with a loss of cell polarity and invasion/metastasis of the mutant tissue, which was not seen with either expression of *Ras*^{ACT} alone in clones or in *scrib*^{1} mutant clones (Brumby and Richardson, 2003; Pagliarini and Xu, 2003). Furthermore, expressing *Ras*^{ACT} in loss-of-function clones of other polarity regulators, such as *dlg*, *lgl*, *baz*, *sdt* and *cdc42*, also resulted in invasive overgrowth (Pagliarini and Xu, 2003), suggesting that loss of polarity combined with Ras^{ACT} is important for cooperative tumorigenesis.

In order to identify other genes that contribute to Ras-mediated tumorigenesis in *Drosophila*, we carried out a dominant modifier genetic screen to identify genes that, when overexpressed, would act like *scrib*^{1} mutants and cooperate with *Ras*^{ACT} (Brumby et al., 2011). Among others, this screen identified the guanine nucleotide exchange factor (GEF) RhoGEF2, an activator of Rho-family GTPases (Barrett et al., 1997; Häcker and Perrimon, 1998; Perrimon

[1]Cell Cycle and Development Laboratory, Research Division, Peter MacCallum Cancer Center, Melbourne, Victoria, Australia
[2]Anatomy and Cell Biology Department, [3]Sir Peter MacCallum Department of Oncology, and [4]Biochemistry and Molecular Biology Department, University of Melbourne, Melbourne, Victoria, Australia
*Author for correspondence (Helena.richardson@petermac.org)

Received 11 April 2012; Accepted 5 January 2013

TRANSLATIONAL IMPACT

Clinical issue

Cancer is a complex disease, involving cooperative interactions between oncogenes and tumour suppressors. A simple model system is needed to dissect the contribution of tumour-promoting mutations to the hallmarks of cancer. The fruit fly, *Drosophila*, is highly suited to the analysis of tumorigenesis owing to its sophisticated genetics, low molecular redundancy and the evolutionary conservation of signalling pathways. This work focuses on Ras-mediated tumorigenesis. The *Ras* oncogene contributes to ~30% of human cancers, but alone is not sufficient for tumorigenesis. Furthermore, Ras-pathway small-molecule inhibitors have proved effective against only a subset of Ras-driven tumours, and resistance often arises. Identifying the factors that cooperate with Ras, and the pathways through which they function in tumorigenesis, is therefore important to improve our understanding of Ras-driven cancers and to reveal new avenues of therapeutic intervention.

Results

In this study, the authors delineated the pathway by which RhoGEF2 cooperates with oncogenic Ras in epithelial tumorigenesis. They provide evidence that RhoGEF2 acts via Rho1, Rok and Myosin II, but does not require Rac1, Limk, Dia or PKN, to upregulate JNK signalling. In addition, Rok–Myosin-II activity was revealed to be necessary and sufficient for Ras-mediated tumorigenesis. The authors observed that activation of Myosin II, which regulates F-actin contractility without affecting F-actin levels, leads to the upregulation of JNK activity and cooperative tumorigenesis with Ras^{ACT}, suggesting that increased F-actin contractility is a key factor in tumour development. They also show that signalling via the Tumour necrosis factor (TNF; also known in *Drosophila* as Egr) ligand is the predominant pathway that activates JNK on Rok activation.

Implications and future directions

This study has revealed a role for F-actin contractility and cell tension, in cooperation with oncogenic Ras, in JNK activation and epithelial tumorigenesis. Although the results implicate an extrinsic mechanism involving TNF-induced JNK signalling, further investigation into the mechanism of JNK activation in *Drosophila* will provide greater mechanistic insights. These findings have the potential to open up new avenues for the development of diagnostics and therapies for Ras-driven human cancers. If it is confirmed that the Rok–myosin-II–JNK pathway is also activated in mammalian Ras-driven tumorigenesis, the phospho-Myosin-II regulatory light-chain antibody would be an ideal biomarker. Moreover, such tumours would be candidates for treatment with Rok or Myosin II small-molecule inhibitors, along with Raf inhibitors.

et al., 1996). Expression of RhoGEF2 enhanced the hyperplastic adult eye phenotype, owing to expression of Ras^{ACT} in the developing eye under the control of the *eyeless-GAL4* driver (*ey* > Ras^{ACT}) (Brumby et al., 2011; Karim and Rubin, 1998). In a clonal setting, overexpression of *RhoGEF2* with Ras^{ACT} in EAD clones resulted in clonal tissue overgrowth through an extended larval stage, cell morphology defects and loss of differentiation. Consistent with the importance of RhoGEF2 in Rho-family activation being important for Ras-mediated tumorigenesis, in the genetic screen we also identified *Rac1* and an activated allele of *Rho1* as cooperating genes with Ras^{ACT} (Brumby et al., 2011). Cooperation was dependent on activation of the JNK pathway: blocking JNK signalling with bsk^{DN} in *RhoGEF2* + Ras^{ACT}-expressing EAD clones suppressed differentiation defects and rescued pupation (Brumby et al., 2011).

The role of RhoGEF2 has been most extensively studied in *Drosophila* embryos. RhoGEF2 was identified from a screen to uncover genes required for embryo patterning (Perrimon et al., 1996) and also from a screen designed to find binding partners of Rho1 (homologue of mammalian RhoA) in the adult eye (Barrett et al., 1997). The structure of RhoGEF2 is that of a typical GEF, containing a DH domain; in addition RhoGEF2 contains a PDZ binding domain and a PH domain, which might be required for subcellular localisation (Häcker and Perrimon, 1998). *RhoGEF2* mutant embryos failed to undergo cell shape changes required for ventral furrow formation during gastrulation (Barrett et al., 1997; Häcker and Perrimon, 1998; Leptin, 1999). This function was linked to Rho1 function, because expression of a dominant negative allele of *Rho1* also displayed similar gastrulation defects. This was confirmed by *in vitro* GDP-GTP exchange assays, which demonstrated that the GEF domain of *RhoGEF2* only significantly catalyses release of GDP from Rho1, but not from Rac, RhoL or Cdc42 proteins (Grosshans et al., 2005). However, whether RhoGEF2 also activates Rac1 *in vivo* in *Drosophila* – as does Pbl, the related RhoGEF (van Impel et al., 2009) – is not known.

Determining the downstream effectors of RhoGEF2-Rho1 or Rac that activate JNK is important for understanding Ras^{ACT}-mediated cooperative tumorigenesis. Extensive analysis in mammalian cells and in *Drosophila* has revealed that Rho1 signals through the effectors Rho kinase (Rok), Protein kinase N (PKN), Lim kinase (Limk) and Diaphanous (Dia) (reviewed by Amano et al., 2010; Jaffe and Hall, 2005; Johndrow et al., 2004; Settleman, 2001). Rok phosphorylates and activates Myosin II regulatory light chain [MRLC; also known as Spaghetti squash (Sqh) and MLC], which in turn activates Myosin II (Zipper), resulting in actin-myosin contraction. Phosphorylation of MLC-phosphatase by Rok inactivates the phosphatase, resulting in increased phosphorylated MRLC. Dia acts with Profilin to promote actin polymerisation. Rok can also phosphorylate Limk, which phosphorylates and inactivates Cofilin, resulting in actin filament (F-actin) stabilisation. PKN modulates cell shape during *Drosophila* embryonic dorsal closure (a sheet epithelial migration that occurs during embryogenesis), and regulates F-actin organisation (Lu and Settleman, 1999; Vincent and Settleman, 1997). The effectors of Rac are P21-activated kinase (PAK), which leads to actin filament stabilisation, PKN (Lu and Settleman, 1999) and WAVE/Scar (Wiskott-Aldrich syndrome protein verprolin homologous), which regulates the Arp2/3 complex, resulting in branched-actin polymerisation (reviewed by Derivery and Gautreau, 2010; Szczepanowska, 2009).

In *Drosophila,* Rho1 can activate JNK via a number of means in different contexts. In the *Drosophila* epithelium, Rho1 mediates apoptosis via JNK activation by forming a complex with a JNK kinase kinase, Slipper (Neisch et al., 2010; Vidal et al., 2006). Furthermore, Rho1 induces JNK-dependent apoptosis and compensatory proliferation in the developing wing epithelium (Warner et al., 2010). *Drosophila* Rac1 can also activate JNK in dorsal closure (Glise and Noselli, 1997; Hou et al., 1997; Woolner et al., 2005). However, in the context of Ras-driven tumorigenesis, how JNK is activated downstream of RhoGEF2 is unknown.

In this study, we investigate which effectors of RhoGEF2 signalling are required for cooperation with Ras^{ACT} in tumorigenesis. We show that Rho1, Rok and Myosin II, but not Rac1, Limk, Dia or PKN, are required for cooperative tumorigenesis with Ras^{ACT} downstream of RhoGEF2. Furthermore, we show that the RhoGEF2–Rho1–Rok–Myosin-II pathway cooperates with

Ras^{ACT} to activate JNK, and that activated Rok or Myosin II is sufficient for cooperation with Ras^{ACT} in tumorigenesis.

RESULTS

RhoGEF2 expression with activated Ras or Raf in clones in the developing EAD results in neoplastic overgrowth

Previously, we have shown that overexpression of *RhoGEF2* + Ras^{ACT} in EAD clones results in clonal tissue overgrowth through an extended larval stage, cell morphology defects and loss of differentiation (Brumby et al., 2011). We had previously found that a gain-of-function allele of the Ras effector protein kinase Raf (Raf^{GOF}) in $scrib^{1}$ clones phenocopied the overgrowth exhibited by $scrib^{1}$ + Ras^{ACT} (Brumby and Richardson, 2003); therefore, we tested whether *RhoGEF2* could also cooperate with Raf^{GOF}. We found that Raf^{GOF} expression was able to cooperate with *RhoGEF2* in a similar manner to Ras^{ACT} (Fig. 1; supplementary material Fig. S1) (Brumby et al., 2011). The mosaic larvae exhibited an extended larval period, and the *RhoGEF2* + Raf^{GOF} tissue [GFP-positive (GFP^{+})] in the EADs overgrew with time (compare Fig. 1A and 1B-D). *RhoGEF2* + Raf^{GOF} tissue contained rounded cells with increased F-actin levels (Fig. 1B, arrowheads; quantified in 1E), as revealed by phalloidin staining (Faulstich et al., 1983), similar to *RhoGEF2*-alone and *RhoGEF2* + Ras^{ACT}-expressing tissues (supplementary material Fig. S1). *RhoGEF2* + Raf^{GOF}-expressing cells showed reduced photoreceptor cell differentiation (Fig. 2A,B), as revealed by staining with the differentiation marker Elav (Robinow and White, 1991). Large undifferentiated GFP^{+} clonal masses were observed in the basal sections of the posterior region of the eye disc (arrow, Fig. 2B). This was similar to *RhoGEF2* + Ras^{ACT} tissue (supplementary material Fig. S1D-F), but was in contrast to what occurs with *RhoGEF2* alone, where cells still differentiate although many are aberrantly localised basally (supplementary material Fig. S1A-C), and to cells expressing Raf^{GOF} (or Ras^{ACT}) alone, which showed ectopic Elav staining (see below) (Brumby et al., 2011). Thus, Raf^{GOF} is sufficient to confer similar tumorigenic effects in cooperation with *RhoGEF2*, as occurs with Ras^{ACT}, showing that cooperation involves the MAPK branch of Ras signalling.

Rho1 is required for *RhoGEF2* + Raf^{GOF} tumorigenesis

We then addressed the issue of which pathways are required downstream of *RhoGEF2* for its cooperation with Ras^{ACT}. *Drosophila* Rho1, the mammalian homologue of RhoA, was previously shown to act downstream of RhoGEF2 during gastrulation (Barrett et al., 1997; Hacker et al., 1998). However, it is not known whether RhoGEF2 activates Rho1 in *RhoGEF2*-expressing clones in the developing EAD or whether Rho1 is required for cooperation of *RhoGEF2* with Ras^{ACT} in tumorigenesis.

First, we investigated whether RhoGEF2 activates Rho1 in the eye disc. We did this by using an active Rho1 reporter (Simões et al., 2006), which contains three binding domains of the Rho1 effector PKN fused to GFP and becomes recruited to the apical membrane by active Rho1 (Rho1-GTP). The localisation and intensity of GFP correlates with active Rho1 activity. When we expressed the Rho1 reporter with *RhoGEF2* in the posterior compartment of eye discs under the control of *GMR-GAL4*, RhoGEF2 was localised apically and greater accumulation of GFP was observed in the apical-lateral region of these cells (arrows,

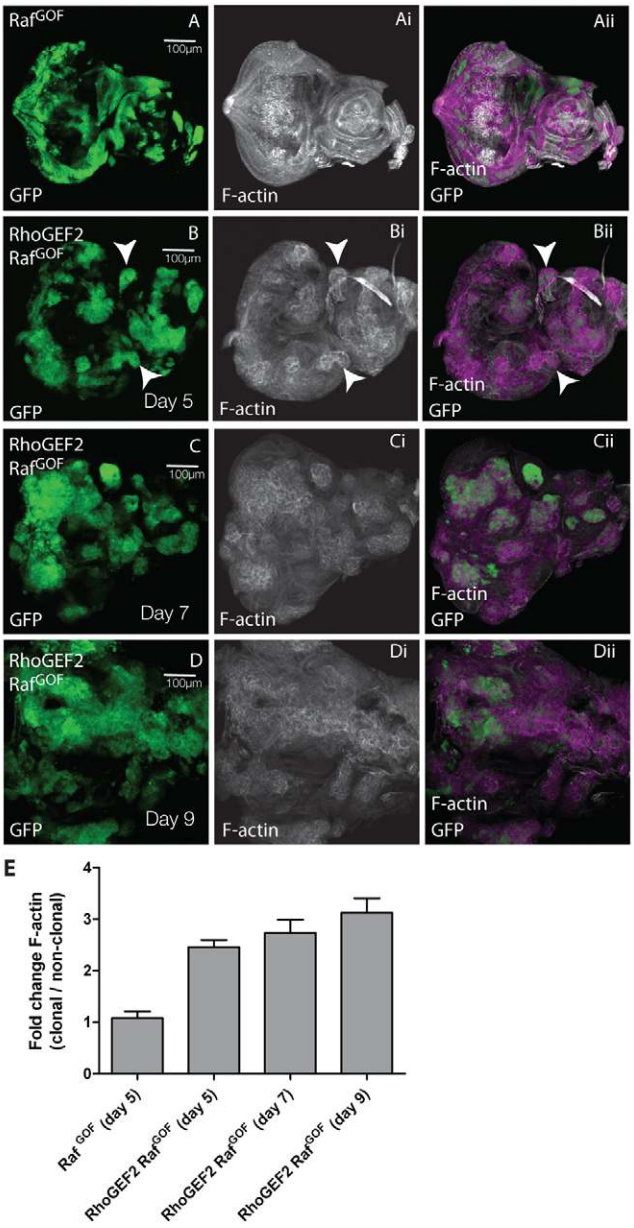

Fig. 1. Co-expression of *RhoGEF2* + Raf^{GOF} in EAD clones results in clonal tissue overgrowth through an extended larval stage. Confocal planar sections through the basal region of the epithelium of third instar larval EADs (A-D). *ey-FLP* was used to induce clones and the mutant tissue is marked by the expression of GFP in all figures unless otherwise indicated. EADs were dissected from wandering third instar larvae at day 5 (A,B), day 7 (C) and day 9 (D) AEL, and stained with phalloidin-TRITC for F-actin (white). Overlap between white and green appears purple in the merges. Images are orientated with anterior to the right in this and all other figures, unless otherwise stated. (A) Raf^{GOF}. (B-D) *RhoGEF2* + Raf^{GOF}. Raf^{GOF} (A) and *RhoGEF2* + Raf^{GOF} (B) mosaic EADs were similar in size at day 5 and similar to control mosaics and *RhoGEF2* mosaic EADs (supplementary material Fig. S1A). Raf^{GOF}-expressing mosaic larvae pupated at day 5, but failed to eclose (data not shown). *RhoGEF2* + Raf^{GOF} EADs increased in size with time (B-D). Both GFP^{+} clonal and wild-type tissue overgrew, but the proportion of GFP^{+} tissue to wild-type tissue increased over time (B-D). In B, arrowheads indicate increased F-actin accumulation. (E) Quantification of F-actin levels in *RhoGEF2* + Raf^{GOF} or Raf^{GOF} clones versus wild-type clones. The data was compared using ANOVA analysis; error bars represent s.e.m. and the significance was $P<0.05$ for *RhoGEF2* + Raf^{GOF} at day 5, 7 or 9 compared with Raf^{GOF} alone.

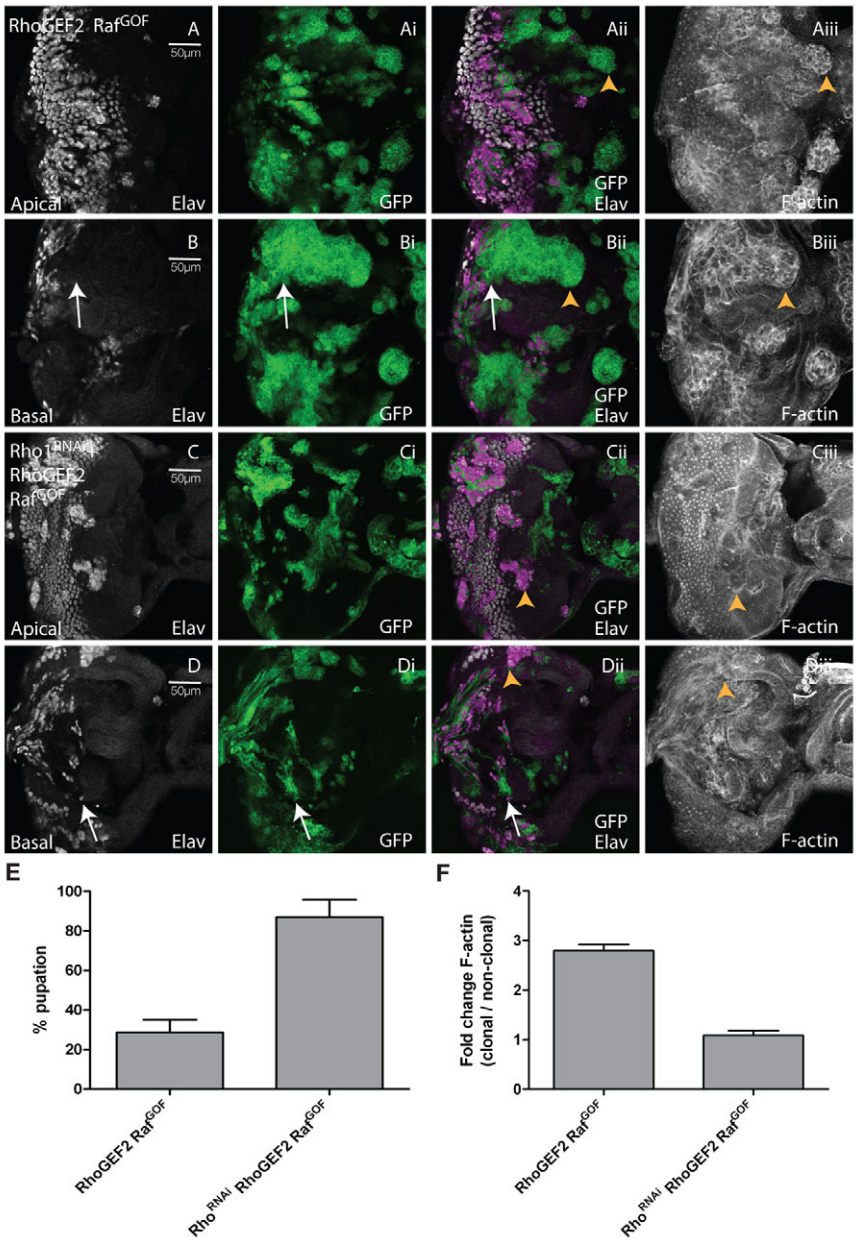

Fig. 2. Reducing levels of Rho1 suppressed clonal tissue overgrowth, differentiation, and cell morphology defects, and rescued pupation in *RhoGEF2 + Raf^{GOF}* EADs. Confocal planar sections through the epithelium of third instar larval EADs. Apical (A,C) and basal (B,D) sections are shown. Mutant tissue was marked by the expression of GFP (green). EADs were stained for Elav (white) and with phalloidin-TRITC for F-actin (white). (A,B) *RhoGEF2 + Raf^{GOF}*. (C,D) *Rho1^{RNAi} +RhoGEF2 + Raf^{GOF}*. Many *RhoGEF2 + Raf^{GOF}*-expressing cells in the posterior region do not stain with Elav, especially in the basal sections of the eye disc, where clonal tissue accumulated (arrows, B-Bii). F-actin was enriched in *RhoGEF2 + Raf^{GOF}*-expressing cells, particularly in basal sections (arrowheads, Aii,Aiii,Bii,Biii). Reducing levels of Rho1 in *RhoGEF2 + Raf^{GOF}*-expressing cells reduced the accumulation of undifferentiated clonal tissue (compare B-Bii with D-Dii, arrows) and reduced F-actin levels (arrowheads, Cii,Ciii,Dii,Diii) compared with *RhoGEF2 + Raf^{GOF}* mosaic EADs (Aii,Aiii,Bii,Biii, arrowheads). (E) Depletion of Rho1 in *RhoGEF2 + Raf^{GOF}* mosaic larvae resulted in increased pupation compared with *RhoGEF2 + Raf^{GOF}* mosaic larvae. The data was compared by a *t*-test and error bars represent s.e.m. The significance was $P<0.0001$. (F) Quantification of F-actin levels in *RhoGEF2 + Raf^{GOF}* or *RhoGEF2 + Raf^{GOF} + Rho1^{RNAi}* clones versus wild-type clones. The data was compared by a *t*-test and error bars represent s.e.m. The significance was $P<0.0001$ for *RhoGEF2 + Raf^{GOF} + Rho1^{RNAi}* versus *RhoGEF2 + Raf^{GOF}*.

supplementary material Fig. S2Bv,Bviii) compared with the control (arrows, supplementary material Fig. S2Aiv,Avi; quantified in S2C). This result indicates that Rho1 is activated by RhoGEF2 in eye disc cells.

To analyse whether Rho1 was functionally required for *RhoGEF2* function, we reduced the levels of Rho1 via expression of a previously validated RNAi transgene (*Rho1^{RNAi}*) (Massarwa et al., 2009; Widmann and Dahmann, 2009; Yan et al., 2009). Expression of *Rho1^{RNAi}* alone in clones did not substantially affect clone size (supplementary material Fig. S3A,B), but resulted in defects in both differentiation and cell morphology; in the posterior region of the eye disc, cells still differentiated but some Elav-positive nuclei were mislocalised basally (arrows, supplementary material Fig. S3B-Bii) and, consistent with this, the pattern of apical foci of F-actin in the posterior region of the eye disc was altered compared with the surrounding wild-type tissue (supplementary material Fig. S3Aiii,Aiv). Expression of *RhoGEF2 + Rho1^{RNAi}* in clones rescued the *RhoGEF2*-clonal phenotype; the small *RhoGEF2* clone size was increased (compare supplementary material Fig. S3Ci and Fig. S1Ai), differentiation was increased (compare supplementary material Fig. S3C with Fig. S1A), cell morphology was improved and F-actin levels were reduced (compare supplementary material Fig. S3Ciii,Civ,Diii,Div and Fig. S1Aii,Bii,Cii; quantified in Fig. S3E). In contrast, knocking down *Rho1* in *Raf^{GOF}*-expressing clones did not substantially alter the *Raf^{GOF}* phenotype (supplementary material Fig. S4); precocious differentiation was still observed (supplementary material Fig. S4C-Cii compared with S4A-Aii), although some differentiated cells were mislocalised basally (arrows, supplementary material Fig. S4D-Dii), as was also observed with *Rho1^{RNAi}* alone and *Raf^{GOF}* alone. However, F-actin levels were not

significantly changed in any sample relative to surrounding wild-type tissue (supplementary material Fig. S4E). Taken together, these results show that Rho1 acts downstream of RhoGEF2, but not Raf^{GOF}, in the developing *Drosophila* EAD.

We then analysed whether Rho1 was required for *RhoGEF2* + Raf^{GOF} tumorigenesis, using $Rho1^{RNAi}$ to knock down Rho1 activity in EAD clones. When levels of Rho1 were reduced in *RhoGEF2* + Raf^{GOF} clones, undifferentiated clonal masses did not accumulate in the basal sections of the eye disc, as was observed for *RhoGEF2* + Ras^{ACT} (arrows, Fig. 2D-Dii, compared with 2B-Bii), differentiation was partially restored as revealed by Elav staining [Fig. 2C-Ciii, 2D-Diii (arrows) compared with 2A-Aiii, 2B-Biii (arrows)] and F-actin levels were significantly reduced (arrowheads, compare Fig. 2Cii,Ciii,Dii,Diii and 2Aii,Aiii,Bii,Biii; quantified in 2F). Importantly, the extended larval period and block to pupation observed for *RhoGEF2* + Raf^{GOF} was suppressed, with a significantly greater proportion of $Rho1^{RNAi}$ + *RhoGEF2* + Raf^{GOF} mosaic larvae pupating compared with *RhoGEF2* + Raf^{GOF} mosaic larvae (Fig. 2E), and no overgrown larvae were observed. Thus, Rho1 is required for the cooperation of *RhoGEF2* with Raf^{GOF}.

Rac1 is not required for *RhoGEF2* + Ras^{ACT} tumorigenesis

Because GEFs can activate multiple GTPases (Rossman et al., 2005) and a dominant negative allele of *Rac1*, $Rac1^{N17}$ ($Rac1^{DN}$) (Baek et al., 2010; Luo et al., 1994) showed partial suppression of *RhoGEF2* + Ras^{ACT} cooperative interactions when expressed throughout the tissue with *ey* > Ras^{ACT} (Brumby et al., 2011), it was possible that RhoGEF2 also acts through Rac. There are three *Drosophila* Rac homologues – *Rac1*, *Rac2* and *Mig-2-like* (*Mtl*), which can act redundantly (Hakeda-Suzuki et al., 2002). To test whether Rac is also required for *RhoGEF2* + Raf^{GOF} cooperation, Rac levels were abrogated by a number of methods (supplementary material Fig. S5). First, we expressed $Rac1^{DN}$, which is thought to block activity of all three Rac homologues (Hakeda-Suzuki et al., 2002), in *RhoGEF2* + Raf^{GOF} clones. Second, Rac1 levels were decreased by expression of a validated RNAi transgene ($Rac1^{RNAi}$) (Baek et al., 2010). Third, Rac1, Rac2 and Mtl levels were reduced by halving the dosage of all three of these genes. When Rac activity was reduced in *RhoGEF2* + Ras^{ACT} clones by expressing $Rac1^{DN}$ or levels of Rac1 were reduced in *RhoGEF2* + Ras^{ACT} clones by expressing $Rac1^{RNAi}$, differentiation in the clones was still significantly reduced at day 5 or 6 after egg laying (AEL) (white arrows, supplementary material Fig. S5B-Bii and 5C-Cii compared with 5A-Aii) in the mutant clones, although there was a small but significant decrease in F-actin in the $Rac1^{RNAi}$-and $Rac1^{DN}$-expressing samples (yellow arrows, supplementary material Fig. S5Biv and 5Civ compared with 5Aiv; quantified in supplementary material Fig. S5E). Similar results were obtained when the dosage of Rac was reduced by halving the dosage of *Rac1*, *Rac2* and *Mtl* in *RhoGEF2* + Ras^{ACT}, except that F-actin levels were not significantly downregulated (supplementary material Fig. S5D,E). Moreover, the block to pupation by *RhoGEF2* + Ras^{ACT} was not rescued by any of these approaches to downregulate Rac activity (data not shown). Thus, these findings show that Rac1 is not required for *RhoGEF2* + Raf^{GOF} cooperative tumorigenesis in EAD clones, which is in agreement with previous biochemical and genetic data that RhoGEF2 activates Rho1, but not Rac1 (Barrett et al., 1997; Grosshans et al., 2005; Häcker and Perrimon, 1998).

Rho kinase is required for *RhoGEF2* + Raf^{GOF} tumorigenesis

Because we showed that Rho1 was required for cooperation of *RhoGEF2* with Raf^{GOF}, we then analysed the downstream effectors Rho1, Rok, Dia, Limk and PKN to determine which of these were required for cooperative tumorigenesis. We knocked down these effectors in *RhoGEF2* + Raf^{GOF} (or Ras^{ACT}) clones, using the previously validated RNAi transgenes rok^{RNAi} (Xu et al., 2008), dia^{RNAi} (Widmann and Dahmann, 2009) and PKN^{RNAi} (Warner and Longmore, 2009). For $Limk^{RNAi}$, we confirmed knock down of the mRNA to 38% by quantitative PCR analysis (data not shown).

Reducing the level of Dia in *RhoGEF2* + Ras^{ACT} clones by the expression of dia^{RNAi} did not restore differentiation in basal sections of the eye disc (arrows, supplementary material Fig. S6B-Bii) or reduce the higher levels of F-actin in *RhoGEF2* + Ras^{ACT}-expressing clones (supplementary material Fig. S6Aiii,Aiv,Biii,Biv; quantified in S6E). Similar effects were observed when PKN^{RNAi} was expressed in *RhoGEF2* + Ras^{ACT}-expressing clones (supplementary material Fig. S6C,D; quantified in S6G), or when $Limk^{RNAi}$ was expressed in *RhoGEF2* + Raf^{GOF}-expressing clones (supplementary material Fig. S6E,F; quantified in S6G). Moreover, the block to pupation by *RhoGEF2* + Ras^{ACT} was not rescued by reducing *dia*, *Limk* or *PKN* levels (data not shown). Thus, Dia, PKN or Limk individually do not play an important role in *RhoGEF2* + Ras^{ACT} (Raf^{GOF}) tumorigenesis.

In contrast, reducing levels of Rok via rok^{RNAi} in *RhoGEF2* + Raf^{GOF} clones rescued the tumorigenic phenotype (Fig. 3). rok^{RNAi} expression alone did not substantially alter clone size or photoreceptor differentiation (supplementary material Fig. S7A-Aii,B-Bii), although produced minor cell morphology defects (arrows, supplementary material Fig. S7Aiii,Aiv). However, reducing Rok in *RhoGEF2* + Raf^{GOF} clones partially restored differentiation in the eye disc clones [compare Fig. 3B,Bi (arrows) and Fig. 2B-Bii] and reduced F-actin accumulation compared with *RhoGEF2* + Raf^{GOF} clones (arrowheads, compare Fig. 3Aii,Aiii,Bii,Biii and Fig. 2Aii,Aiii,Bii,Biii; quantified in Fig. 3F). Furthermore, knockdown of Rok in *RhoGEF2* + Raf^{GOF} clones rescued the pupation defect of *RhoGEF2* + Raf^{GOF} (Fig. 3E). Thus, Rok is required for *RhoGEF2* + Raf^{GOF} tumorigenesis.

To explore how Rok contributed to *RhoGEF2* + Raf^{GOF} tumorigenesis, we examined whether rok^{RNAi} affected Raf^{GOF} as well as *RhoGEF2* phenotypes. As expected, expression of rok^{RNAi} with *RhoGEF2* in clones rescued the small clone size (compare Fig. 3C,D and supplementary material Fig. S1Ai,Bi), the differentiation defects (compare Fig. 3C-Cii,D-Dii and supplementary material Fig. S1A,Ai,B,Bi,Ci,Cii), the cell morphology defects and the elevated F-actin levels of *RhoGEF2* (compare Fig. 3Ciii,Diii and supplementary material Fig. S1Aii,Aiii,Bii,Biii,Cii,Ciii; quantified in Fig. 3F). However, expression of rok^{RNAi} in Raf^{GOF} clones did not substantially alter the Raf^{GOF} phenotype; precocious Elav-positive cells were still observed anterior to the morphogenetic furrow (MF; arrows, supplementary material Fig. S7C-Cii) and some differentiated cells were present in the basal sections of the eye disc (arrows, supplementary material Fig. S7D-Dii), but F-actin levels were not affected compared with the surrounding wild-type tissue (supplementary material Fig. S7Ciii,Civ,Diii,Div,E). Thus, Rok is required for the *RhoGEF2*, but not the Raf^{GOF}, phenotypes.

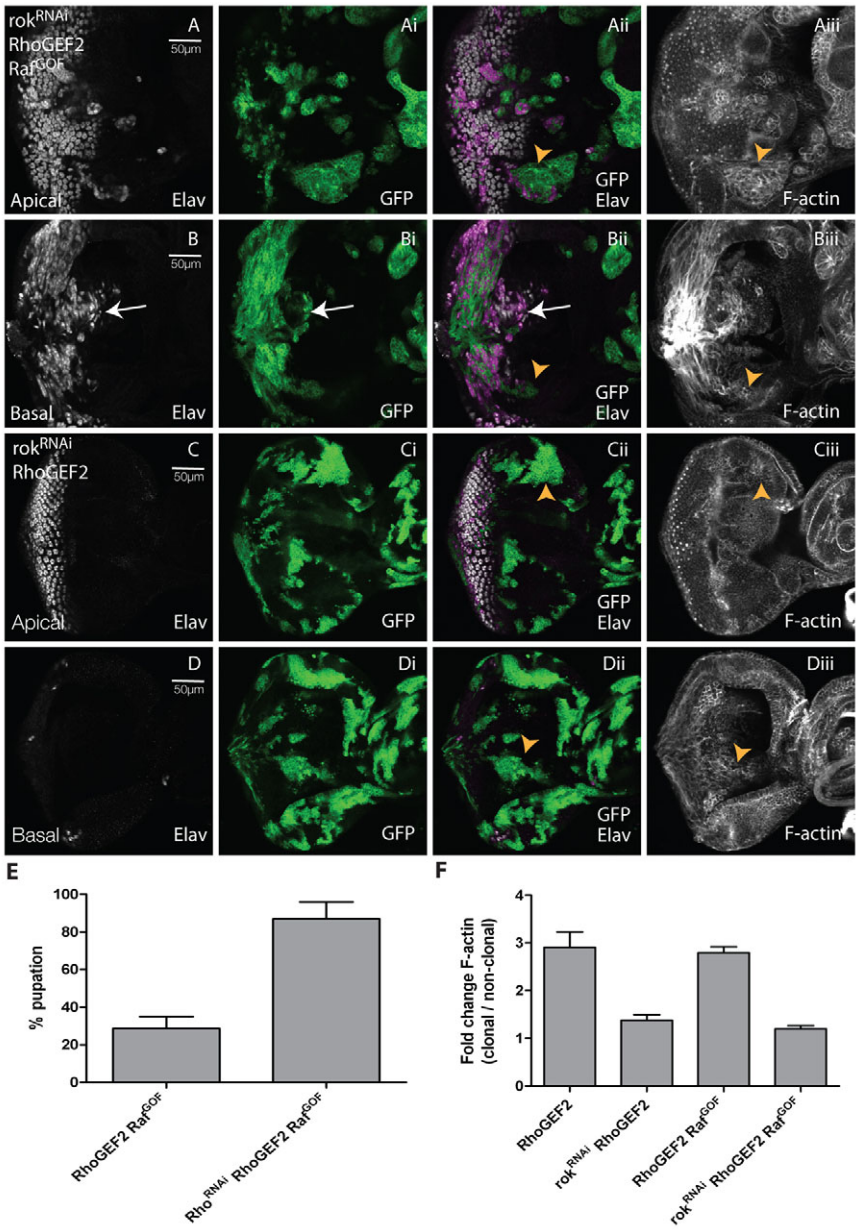

Fig. 3. Reducing levels of Rok in *RhoGEF2* + *Raf*^{GOF} co-expressing EAD clones suppressed clonal tissue accumulation, differentiation and cell morphology defects, and rescued pupation. Confocal planar sections through the epithelium of day 5 AEL third instar larval EADs. Apical (A,C) and basal (B,D) sections are shown. Mutant tissue was marked by the expression of GFP (green). EADs were stained for Elav (white) and with phalloidin-TRITC for F-actin (white). (A,B) *rok*^{RNAi} + *RhoGEF2* + *Raf*^{GOF}. (C,D) *rok*^{RNAi} + *RhoGEF2*. Expression of *rok*^{RNAi} in *RhoGEF2* + *Raf*^{GOF} clones resulted in reduced accumulation of undifferentiated clonal tissue compared with *RhoGEF2* + *Raf*^{GOF} mosaic eye discs (compare arrows, B-Bii and Fig. 2B-Bii) and reduced the high levels of F-actin in the mutant cells (arrowheads in Aiii,Biii compared with Fig. 2Aii,Aiii,Bii,Biii). *rok*^{RNAi} in *RhoGEF2* clones rescued the reduced clone size, F-actin accumulation and morphology defects of *RhoGEF2*-alone clones (arrowheads in Cii,Ciii,Dii,Diii compared with supplementary material Fig. S1Aii,Aiii,Bii,Biii). Note that the high levels of F-actin observed in Biii are due to the axonal projections that are present in this basal section. (E) Expression of *rok*^{RNAi} in *RhoGEF2* + *Raf*^{GOF}-expressing cells resulted in an increase in pupation compared with *RhoGEF2* + *Raf*^{GOF} expression alone. The data was compared by a *t*-test and error bars represent s.e.m. The significance was $P<0.0001$. (F) Quantification of F-actin levels in *RhoGEF2* + *Raf*^{GOF} + *rok*^{RNAi} or *RhoGEF2* + *rok*^{RNAi} clones versus wild-type clones. The data was compared by a *t*-test and error bars represent s.e.m. The significance was $P<0.0004$ for *RhoGEF2* + *rok*^{RNAi} versus *RhoGEF2* and $P<0.0001$ for *RhoGEF2* + *Raf*^{GOF} + *Rho1*^{RNAi} versus *RhoGEF2* + *Raf*^{GOF}.

Myosin II is required for *RhoGEF2* + *Raf*^{GOF} tumorigenesis

Given the finding that Rok suppressed *RhoGEF2* + *Raf*^{GOF} cooperation, we then sought to examine which effectors downstream of Rok are required. Mammalian Rok can act via activation of Limk and MRLC (Amano et al., 2010). In *Drosophila*, Rok has not been shown to regulate Limk, but phosphorylates the *Drosophila* MRLC (Winter et al., 2001), encoded by *sqh* (Jordan and Karess, 1997), which in turn activates Myosin II heavy chain, encoded by *zipper* (*zip*) (Young et al., 1993), to regulate cell contractility. Furthermore, RhoGEF2 regulates actin-myosin contractility during gastrulation through Rho1, Rok and Zip (Barrett et al., 1997; Dawes-Hoang et al., 2005; Hacker et al., 1998), and *RhoGEF2* and *zip* genetically interact in leg imaginal disc morphogenesis (Halsell et al., 2000).

Because we have already ruled out the involvement of Limk for *RhoGEF2* + *Raf*^{GOF} cooperation (see supplementary material Fig. S6E,F), we examined whether Myosin II was required. We knocked down Myosin II activity with a previously validated *zip*^{RNAi} transgene (Kwon et al., 2010) in *RhoGEF2* + *Raf*^{GOF} clones and assessed the effect on differentiation and cell morphology. Expression of *zip*^{RNAi} alone resulted in a slight reduction in clone size relative to wild-type clones, and in some defects in differentiation and cell morphology (supplementary material Fig. S8A-Aii and arrows in S8B-Bii). However, Myosin II depletion in *RhoGEF2* + *Raf*^{GOF} clones partially restored differentiation compared with *RhoGEF2* + *Raf*^{GOF}-expressing mosaic eye discs (compare Fig. 4B-Bii and Fig. 2B-Bii), and suppressed the cell morphology and elevated F-actin defects of the mutant tissue (compare Fig. 4Aii,Aiii,Bii,Biii and Fig. 2Aii,Aiii,Bii,Biii; quantified in Fig. 4F). Moreover, reducing Myosin II levels rescued the pupation defect of *RhoGEF2* + *Raf*^{GOF} larvae (Fig. 4E). Thus, Myosin II is required for *RhoGEF2* + *Raf*^{GOF} tumorigenesis.

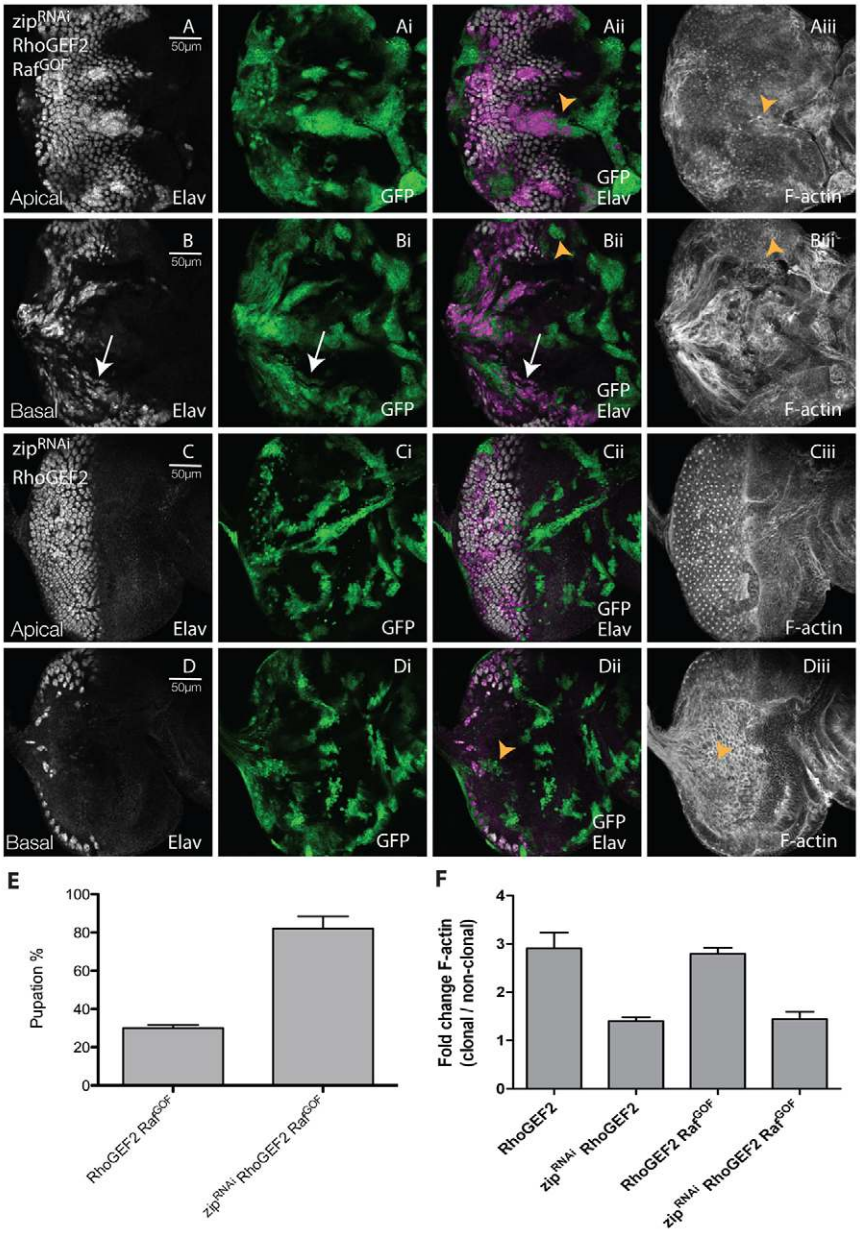

Fig. 4. Reducing levels of Myosin II (Zip) in *RhoGEF2* + *Raf^{GOF}*-expressing EAD clones suppressed clonal tissue accumulation, differentiation, and cell morphology defects, and restored pupation. Confocal planar sections through the epithelium of day 5 AEL third instar larval EADs. Apical (A,C) and basal (B,D) sections are shown. Mutant tissue was marked by the expression of GFP (green). EADs were stained for Elav (white) and with phalloidin-TRITC for F-actin (white). (A,B) *zip^{RNAi}* + *RhoGEF2* + *Raf^{GOF}*. (C,D) *zip^{RNAi}* + *RhoGEF2*. Expression of *zip^{RNAi}* in *RhoGEF2* + *Raf^{GOF}* co-expressing cells resulted in reduced accumulation of undifferentiated clonal tissue basally compared with *RhoGEF2* + *Raf^{GOF}* mosaic eye discs (compare arrows in B-Bii and Fig. 2B-Bii) and reduced F-actin accumulation in the mutant cells (compare arrowheads in Aii,Aiii,Bii,Biii and Fig. 2Aii,Aiii,Bii,Biii). (C,D) *zip^{RNAi}* in *RhoGEF2* clones rescued the reduced clone size, F-actin accumulation and morphology defects of *RhoGEF2*-alone clones (arrowheads in Dii,Diii compared with supplementary material Fig. S1Bii,Biii). (E) Expression of *zip^{RNAi}* in *RhoGEF2* + *Raf^{GOF}*-expressing cells resulted in an increase in pupation compared with *RhoGEF2* + *Raf^{GOF}* expression alone. The data was compared by a *t*-test and error bars represent s.e.m. The significance was $P<0.0001$. (F) Quantification of F-actin levels in *RhoGEF2* + *Raf^{GOF}* + *zip^{RNAi}* or *RhoGEF2* + *zip^{RNAi}* clones versus wild-type clones. The data was compared by a *t*-test and error bars represent s.e.m. The significance was $P<0.0001$ for *RhoGEF2* + *zip^{RNAi}* compared with *RhoGEF2* and for *RhoGEF2* + *Raf^{GOF}* + *zip^{RNAi}* compared with *RhoGEF2* + *Raf^{GOF}*.

To determine how Myosin II knockdown was affecting *RhoGEF2* + *Raf^{GOF}* tumorigenesis, we examined its affect on the *RhoGEF2* or *Raf^{GOF}* phenotypes alone. As expected, knockdown of Myosin II in *RhoGEF2*-expressing clones rescued the clone size relative to *RhoGEF2* alone (compare Fig. 4Ci,Di and supplementary material Fig. S1Ai,Bi). The differentiation defects were also partially rescued (compare Fig. 4C and supplementary material Fig. S1A,B), as was the cell morphology defects and F-actin accumulation (compare Fig. 4Ciii,Diii and supplementary material Fig. S1Aii,Bii,Cii; quantified in Fig. 4F). In contrast, knockdown of Myosin II did not alter the *Raf^{GOF}* phenotype; ectopic differentiation was still observed anterior to the MF (arrows, supplementary material Fig. S8C-Cii) and some photoreceptor nuclei were basally localised (arrows, supplementary material Fig. S8D-Dii), but F-actin levels were not affected compared with the surrounding wild-type tissue (supplementary material Fig. S8E). Thus, Myosin II is required for the *RhoGEF2*, but not the *Raf^{GOF}*, phenotypes.

The Rho1–Rok–Myosin-II pathway contributes to the upregulation of JNK in *RhoGEF2*-expressing clones

We have previously shown that JNK is upregulated and required for *RhoGEF2* + *Ras^{ACT}* tumorigenesis (Brumby et al., 2011). Because our results here have shown that cooperation of *RhoGEF2* with *Ras^{ACT}* depends on Rho1, Rok and Myosin II, we then investigated whether this pathway also contributes to JNK upregulation in *RhoGEF2*-expressing clones (Fig. 5). Expression of *RhoGEF2* resulted in upregulation of the JNK reporter *msn-lacZ* (Mattila et al., 2005) in some cells, which was most obvious in clones in the anterior-lateral regions of the eye disc (arrows, Fig. 5A-Aii). When levels of Rho1 or Zip were reduced in *RhoGEF2*-expressing clones, *msn-lacZ* expression was still detectable in the lateral region

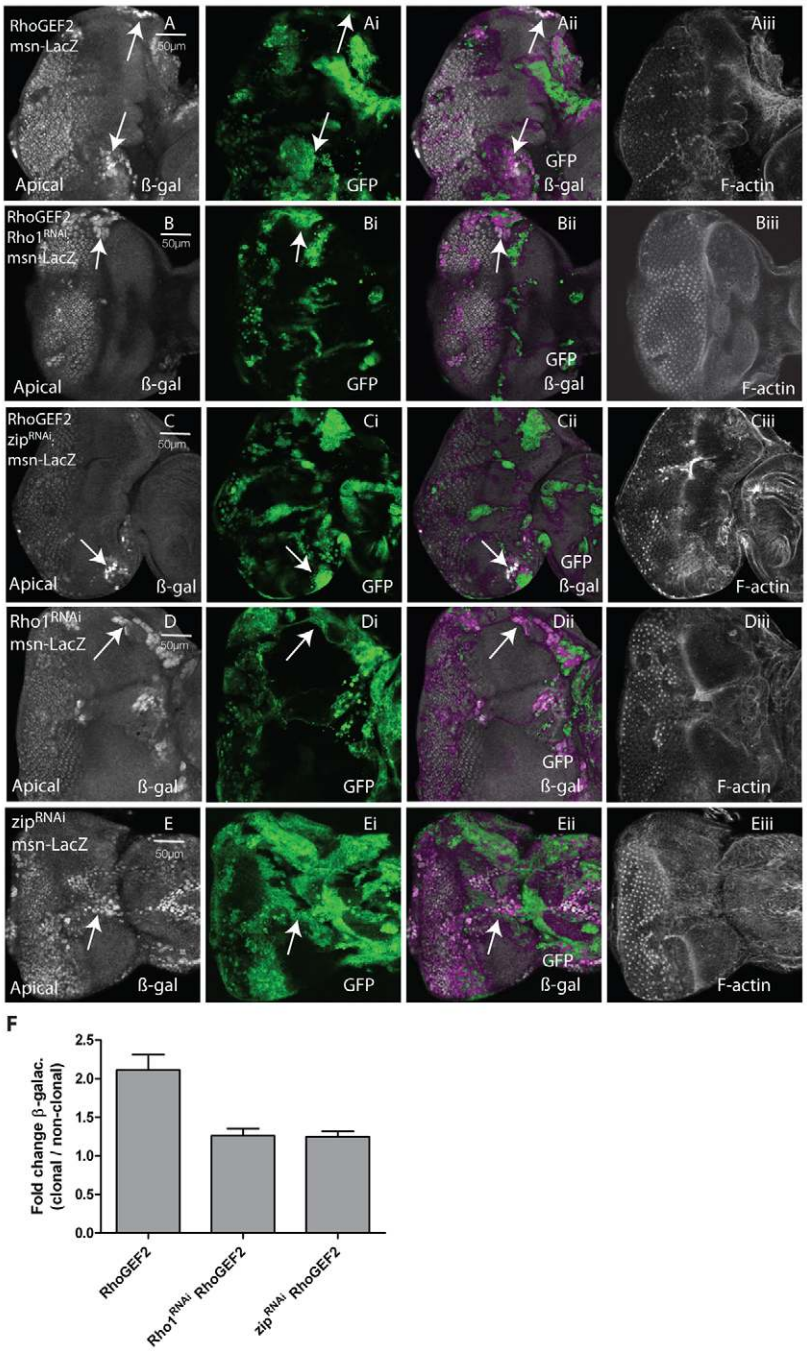

Fig. 5. Knockdown of Rho1 or Myosin II (Zipper) in *RhoGEF2* EAD clones resulted in partial suppression of the JNK pathway activation. Confocal planar sections through the epithelium of third instar larval EADs. Mutant tissue was marked by the presence of GFP (green). JNK activity was detected by *msn-lacZ* enhancer trap expression, marked by β-galactosidase (β-gal) staining (white). (A) *RhoGEF2 msn-lacZ*. (B) $Rho1^{RNAi}$ + *RhoGEF2 msn-lacZ*. (C) zip^{RNAi} + *RhoGEF2 msn-lacZ*. (D) $Rho1^{RNAi}$ *msn-lacZ*. (E) zip^{RNAi} *msn-lacZ*. Compared with the control, *msn-lacZ* was upregulated in some *RhoGEF2*-expressing cells, particularly in the lateral regions of the EAD, indicating JNK pathway activation (arrows, A-Aii). Reducing levels of Rho1 or Zip by expressing $Rho1^{RNAi}$ or zip^{RNAi} in *RhoGEF2*-expressing cells partially suppressed either the intensity of, or number of cells with, *msn-lacZ* expression (arrows, B-Bii,C-Cii). Expression of $Rho1^{RNAi}$ or zip^{RNAi} in clones resulted in upregulation of *msn-lacZ* in the lateral regions of the eye disc (arrows, D-Dii,E-Eii). Note that, in E, the eye disc is folded and the arrow is pointing to the lateral edge. (F) Quantification of the level of *msn-lacZ* staining in *RhoGEF2*-, $Rho1^{RNAi}$ + *RhoGEF2*- or zip^{RNAi} + *RhoGEF2*-expressing clones in the lateral regions of the eye disc relative to adjacent wild-type clones. This reflects the intensity of staining as well as the number of cells that are positive for *msn-lacZ*. The data was compared using ANOVA analysis; error bars represent s.e.m. and the significance was $P<0.05$ for $Rho1^{RNAi}$ + *RhoGEF2* compared with *RhoGEF2* and for zip^{RNAi} + *RhoGEF2* compared with *RhoGEF2*.

clones, but was significantly reduced relative to *RhoGEF2* expression alone, reflecting a decrease in either the number of expressing cells or in the level of expression (arrows, Fig. 5B-Bii,C-Cii; quantified in 5F). However, *msn-lacZ* expression was upregulated when $Rho1^{RNAi}$ or zip^{RNAi} were expressed alone in clones (arrows, Fig. 5D-Dii,E-Eii), perhaps owing to a disruption of cell morphology. This suggests that the JNK activation still observed in *RhoGEF2*-expressing clones upon $Rho1^{RNAi}$ or zip^{RNAi} expression might be due to the depletion of Rho1 or Myosin II to below normal levels. Taken together, these data show that activation of Rho1 and Myosin II contributes to JNK pathway activation in *RhoGEF2*-expressing EAD clones.

Activation of Rok or Myosin II is sufficient for Ras^{ACT}-mediated cooperative tumorigenesis

Having shown the importance of Rok and Myosin II downstream of RhoGEF2 in cooperative tumorigenesis with Ras^{ACT}, we then sought to investigate whether upregulation of Rok or Myosin II was sufficient for tumorigenesis. Therefore, we expressed constitutively active versions of *rok* [rok^{CAT} (Verdier et al., 2006)] or *MRLC* [sqh^{EE} (Wang and Riechmann, 2007)] in clones alone or with Ras^{ACT} (Figs 6, 7).

Expression of rok^{CAT} alone in clones did not substantially affect clone size compared with wild type, but showed mild disruption to differentiation, with Elav-positive cells detected in basal

sections (arrows, Fig. 6A-Aii,B-Bii). Morphological defects were also apparent, although F-actin was not significantly upregulated (Fig. 6Aiii,Aiv and arrowheads in Biii,Biv; quantified in 6F). When rok^{CAT} was expressed with Ras^{ACT}, cooperative tumorigenesis occurred, leading to a blockage to pupation (reduced to ~30%; Fig. 6E) similar to that caused by *RhoGEF2* + Raf^{GOF} (or Ras^{ACT}) (Fig. 2E; and data not shown). Massive tumours developed over an extended larval stage, similar to *RhoGEF2* + Ras^{ACT} (or Raf^{GOF}) (supplementary material Fig. S9; and data not shown). Analysis of the EADs revealed an accumulation of mutant tissue basally, reduced differentiation (Fig. 6Ci,Cii and arrows in 6Di,Dii) and morphological defects with accumulation of F-actin (Fig. 6Ciii,Civ and arrowheads in 6Diii,Div; quantified in 6F). Thus, rok^{CAT} cooperates with Ras^{ACT} similarly to *RhoGEF2* with Ras^{ACT}.

When we expressed the activated version of *sqh* alone in clones, no substantial effect on clone size, differentiation or cell morphology was observed (Fig. 7A,B). However, when sqh^{EE} was expressed with Ras^{ACT} in clones, cooperative tumorigenesis was observed, with large masses of undifferentiated clonal tissue present in basal sections of eye discs and reduced differentiation (arrowheads, Fig. 7D-Dii). However, in contrast to rok^{CAT} + Ras^{ACT} or *RhoGEF2* + Ras^{ACT}, F-actin levels were not significantly upregulated in day 5/6 larval EAD clones (compare Fig. 7Ciii,Civ,Diii,Div and Fig. 6Ciii,Civ,Diii,Div and supplementary material Fig. S1Dii,Diii,Eii,Eiii,Fii,Fiii; quantified in Fig. 7F). Despite not showing a significant effect on F-actin upregulation, sqh^{EE} showed robust cooperation with Ras^{ACT}, resulting in massive tumour overgrowth over an extended larval stage (supplementary material Fig. S10), and reduced pupation

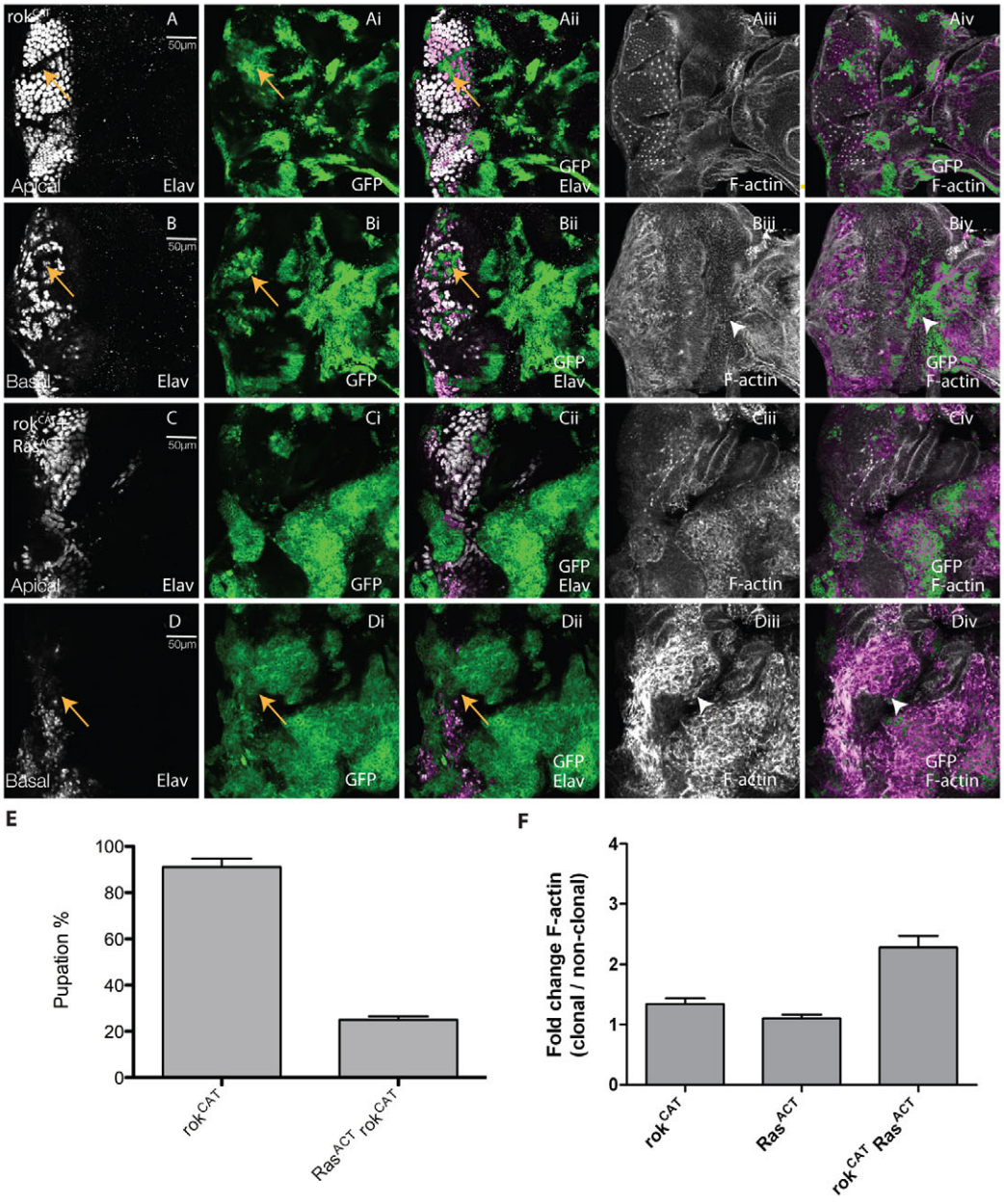

Fig. 6. Expression of activated *rok* with Ras^{ACT} leads to clonal tissue overgrowth and reduced pupation. Apical or basal confocal planar sections through the epithelium of third instar larval EADs (A-D). Mutant tissue was marked by the expression of GFP (green). EADs were stained for Elav (white) and with phalloidin-TRITC for F-actin (white). (A,B) rok^{CAT}. (C,D) rok^{CAT} + Ras^{ACT}. Expression of rok^{CAT} resulted in disruption to the pattern of differentiation (arrows, A-Aii). Some rok^{CAT}-expressing $Elav^{+}$ cells were basally localised (arrows, B-Bii). However, unlike *RhoGEF2*-expressing clones, F-actin was not upregulated in rok^{CAT}-expressing clones (arrowheads, Biii and Biv) compared with adjacent wild-type tissue. Expression of rok^{CAT} + Ras^{ACT} in clones resulted in large masses of undifferentiated clonal tissue (arrows, D-Dii) particularly in basal sections of EADs and upregulation of F-actin in the clones (Ciii,Civ and arrowheads in Diii-Div), similar to *RhoGEF2* + Ras^{ACT} expression (supplementary material Fig. S1Dii,Diii,Eii,Eiii). (E) Expression of rok^{CAT} + Ras^{ACT} resulted in decreased pupation compared with rok^{CAT} expression alone. The data was compared by a *t*-test and error bars represent s.e.m. The significance was $P<0.0001$. (F) Quantification of F-actin levels in rok^{CAT} + Ras^{ACT} or rok^{CAT} clones versus wild-type clones. The data was compared using ANOVA analysis and error bars represent s.e.m. The significance was $P<0.05$ for rok^{CAT} + Ras^{ACT} versus rok^{CAT} and for rok^{CAT} + Ras^{ACT} versus Ras^{ACT}.

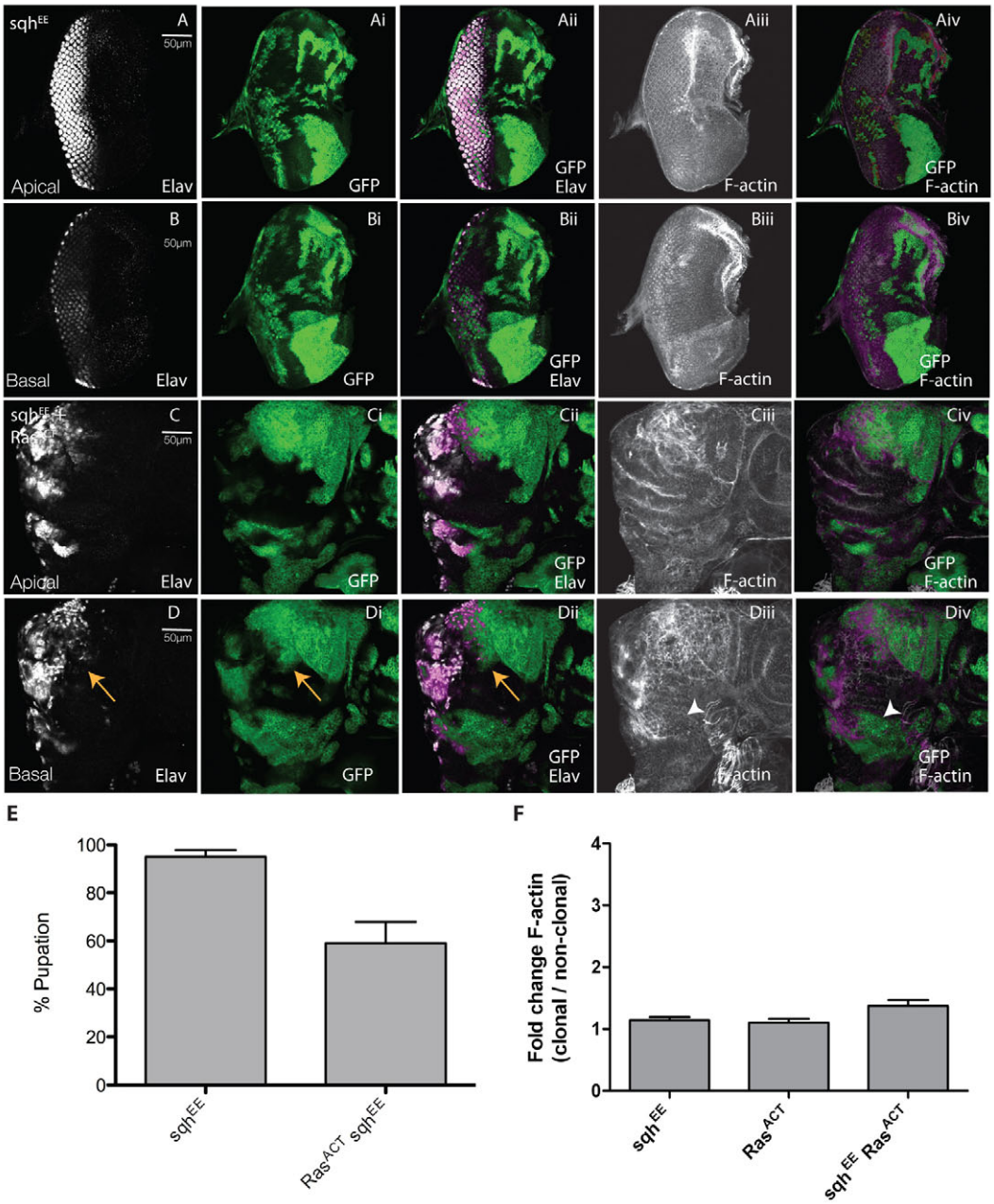

Fig. 7. Expression of activated Myosin II regulatory light chain (Sqh) with Ras^{ACT} leads to clonal tissue overgrowth and decreased pupation. Apical or basal confocal planar sections through the epithelium of third instar larval EADs (A-D). Mutant tissue was marked by the expression of GFP (green). EADs were stained for Elav (white) and with phalloidin-TRITC for F-actin (white). (A,B) sqh^{EE}. (C,D) sqh^{EE} + Ras^{ACT}. Expression of sqh^{EE} did not noticeably affect differentiation or cell morphology (A,B). When sqh^{EE} was expressed with Ras^{ACT} in clones (C,D), large masses of undifferentiated clonal tissue were observed in basal sections of eye discs (arrows, D-Dii), although F-actin levels were not substantially upregulated (Ciii,Civ and arrowheads in Diii-Div). (E) Expression of sqh^{EE} + Ras^{ACT} resulted in decreased pupation compared with sqh^{EE} expression alone. The data was compared by a *t*-test and error bars represent s.e.m. The significance was $P<0.05$. (F) Quantification of F-actin levels in sqh^{EE} + Ras^{ACT} or sqh^{EE} clones versus wild-type clones. The data was compared using ANOVA analysis and error bars represent s.e.m. The significance was $P<0.05$ for sqh^{EE} + Ras^{ACT} versus Ras^{ACT}.

(reduced to ~60%; Fig. 7E), which, although not as strongly reduced as with *RhoGEF2* + Raf^{GOF} (or Ras^{ACT}) (Fig. 2E; and data not shown), was still significantly decreased. Thus, activation of Myosin II is sufficient for cooperation with Ras^{ACT}. Furthermore, because F-actin was not upregulated in sqh^{EE} + Ras^{ACT} tissue at least at the early stages of tumorigenesis, this suggests that cooperative tumorigenesis initiates independently of increased F-actin levels.

Activated Rok and Myosin II cooperate with Ras^{ACT} to activate JNK

We then tested the effect of activated Rok and Myosin II on JNK pathway activation, using the expression of a JNK target, Mmp1 (Uhlirova and Bohmann, 2006). Expression of rok^{CAT} did not upregulate Mmp1 in the majority of EADs, although it was weakly upregulated in some clones (Fig. 8A; quantified in 8F). However, Mmp1 was strongly upregulated in rok^{CAT} + Ras^{ACT} clones (Fig. 8C; quantified in 8F), whereas Ras^{ACT} clones alone did not substantially upregulate Mmp1 in the majority of EADs (Fig. 8B). Similarly, sqh^{EE} expression alone did not upregulate Mmp1 (Fig. 8D; quantified in 8F); however, Mmp1 was robustly upregulated in some sqh^{EE} + Ras^{ACT} clones (Fig. 8E,F). Taken together, these results show that activation of Rok or Myosin II cooperates with Ras^{ACT} to induce JNK activation. Although we did not detect significant effects on Mmp1 upregulation in rok^{CAT} or sqh^{EE} clones alone, since Mmp1 is a weaker reporter of JNK pathway activation compared with *msn-lacZ* (data not shown), JNK activity might be induced at low levels by Rok or Myosin II activation.

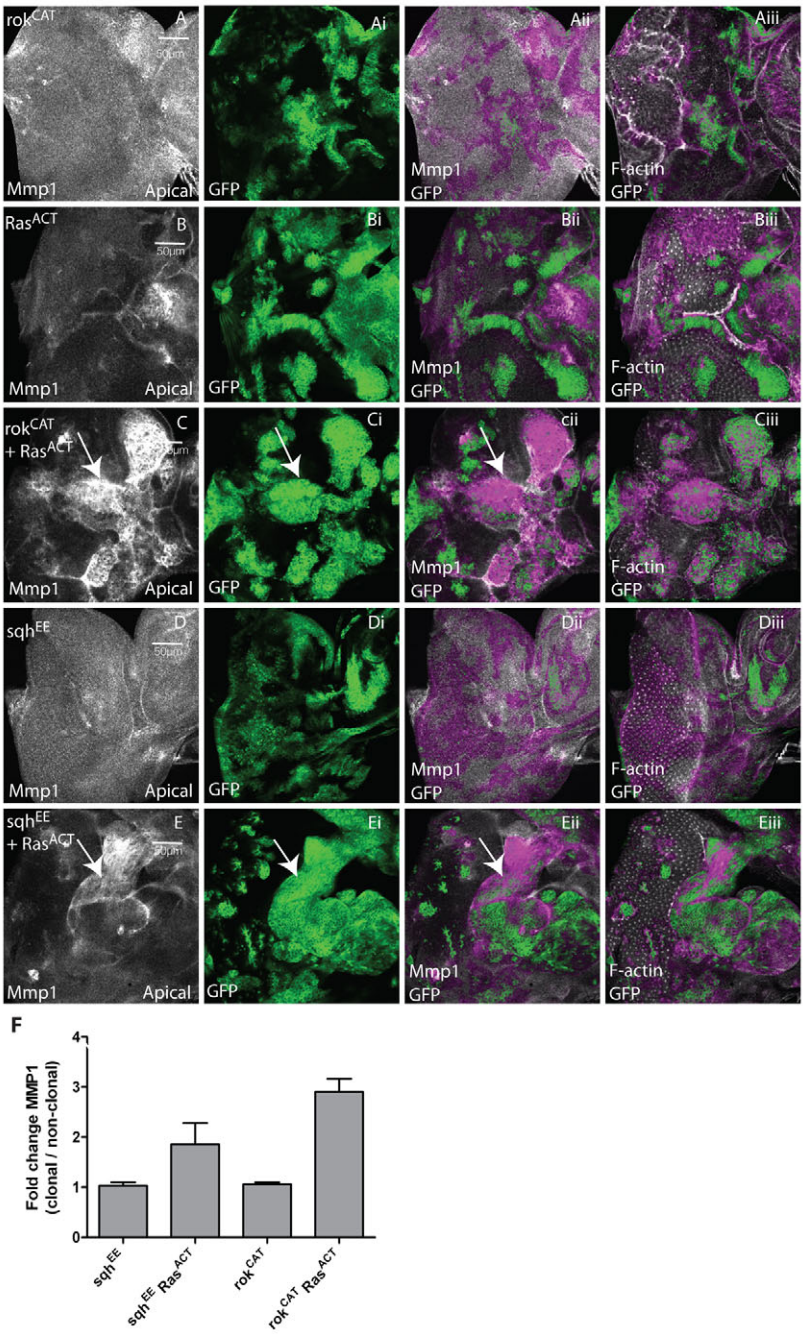

Fig. 8. Activation of Rok and Myosin II lead to increased expression of the JNK target Mmp1 in EAD clones. Confocal planar apical sections through the epithelium of third instar larval EADs. Mutant clones are marked by the presence of GFP (green). EADs were stained for Mmp1 to reveal JNK activity (white) and with phalloidin-TRITC to detect F-actin (white). (A) rok^{CAT}. (B) Ras^{ACT}. (C) rok^{CAT} + Ras^{ACT}. (D) sqh^{EE}. (E) sqh^{EE} + Ras^{ACT}. Third instar EADs from rok^{CAT} mosaic larvae did not show upregulation of Mmp1 in the majority of clones, although expression was mildly induced in some clones (not shown). Expression of Ras^{ACT} alone did not upregulate Mmp1 in the majority of clones. Mmp1 was strongly upregulated in most rok^{CAT} + Ras^{ACT} clones (arrows, C-Cii) compared with adjacent wild-type tissue. Expression of sqh^{EE} did not lead to Mmp1 upregulation in the clones (D), whereas expression of sqh^{EE} + Ras^{ACT} resulted in induction of Mmp1 in many but not all clones (arrows, E-Eii). (F) Quantification of Mmp1 levels in sqh^{EE}, sqh^{EE} + Ras^{ACT}, rok^{CAT} or rok^{CAT} + Ras^{ACT} clones versus wild-type clones. The data was compared by a *t*-test and error bars represent s.e.m. The significance was $P<0.0001$ for rok^{CAT} + Ras^{ACT} compared with rok^{CAT} and $P<0.08$ for sqh^{EE} + Ras^{ACT} compared with sqh^{EE}.

How is JNK upregulated by the RhoGEF2–Rho1–Rok–Myosin-II pathway in cooperation with Ras^{ACT}?

Recent studies have revealed an extrinsic mechanism by which JNK is activated during tumorigenesis in the developing *Drosophila* wing or EAD epithelia, involving exogenous activation of JNK via the tumour necrosis factor (TNF) homologue Eiger (Egr) (Cordero et al., 2010; Igaki et al., 2009; Ohsawa et al., 2011). JNK activation and induction of apoptosis in *scrib* mutant clones is dependent on Egr, which is produced by circulating haemocytes (macrophage-like cells) to induce JNK upregulation in the *scrib* mutant cells, leading to their elimination through apoptosis (Cordero et al., 2010; Igaki et al., 2009; Lolo et al., 2012; Ohsawa et al., 2011). How the *scrib* mutant cells are recognised is currently unknown, but might involve changes in cell morphology. Similarly, the change in cell morphology in rok^{CAT} clones might trigger such a pathway. *scrib* mutant clones in the EAD are smaller than wild-type clones due to JNK-mediated cell death (Brumby and Richardson, 2003), but in a homozygous *egr* mutant background the small clone size is rescued owing to blockage of JNK-mediated apoptosis (Cordero et al., 2010; Igaki et al., 2009). rok^{CAT} clones are not significantly smaller than wild-type clones (Fig. 9A,B,E); however, they also show increased cell death, as revealed by TUNEL staining (Fig. 9B compared with the control in 9A). Most apoptosis was cell autonomous; however, some apoptotic cells were also observed in the surrounding wild-type cells. To investigate whether the increased cell death in the rok^{CAT} mosaic EADs was due to Egr

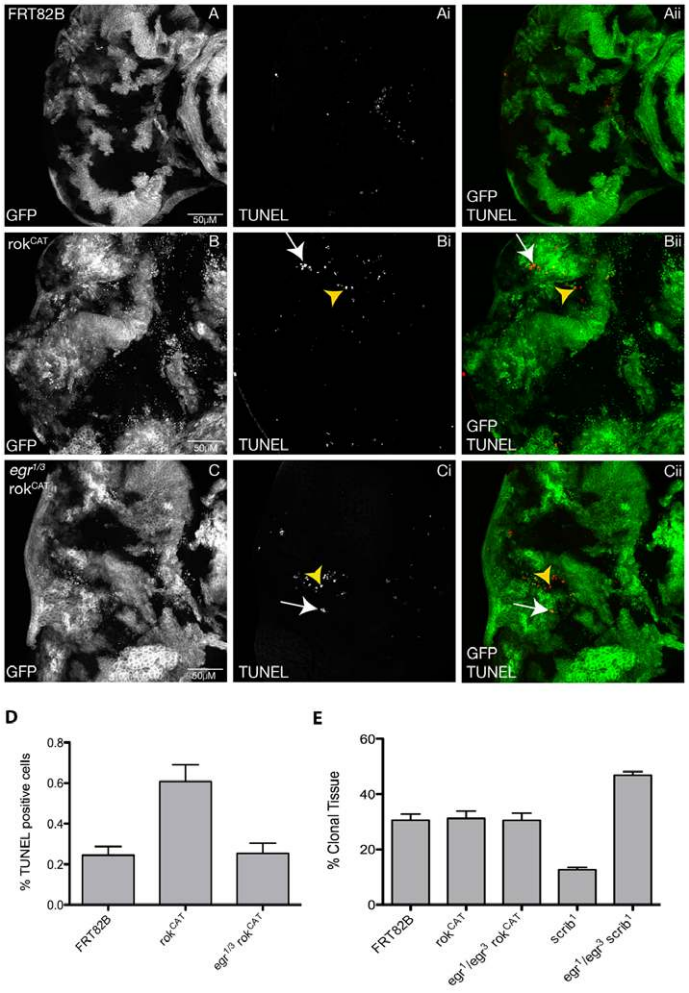

Fig. 9. TNF (Eiger) is required for apoptosis in *rok*^{CAT} clones. Confocal planar compiled sections through the epithelium of third instar larval EADs. Mutant clones are marked by the presence of GFP (white, and green in the merge) and TUNEL (white, and red in the merge). (A) *FRT82B* control. (B) *rok*^{CAT}. (C) *egr*$^{1/3}$ *rok*^{CAT}. Third instar EADs from *rok*^{CAT} mosaic larvae show higher levels of apoptotic cells, as revealed by TUNEL, both cell autonomously (arrows, Bi,Bii) and non-cell autonomously (arrowheads, Bi,Bii). Removing *egr* reduced, but did not eliminate, apoptotic cells in the *rok*^{CAT} EAD in both *rok*^{CAT} (arrows, Ci,Cii) and wild-type clones (arrowheads, Ci,Cii). (D) Quantification of the number of TUNEL-positive cells in EADs of each genotype indicated. The data was compared by a *t*-test and error bars represent s.e.m. The significance was $P<0.05$ for *rok*^{CAT} compared with the *FRT* control, and for *rok*^{CAT} compared with *egr*$^{1/3}$ *rok*^{CAT}. (E) Quantification of the percentage of mutant clonal tissue relative to the total EAD size for each genotype indicated. The data was compared by a *t*-test and error bars represent s.e.m. The significance was $P<0.05$ for *scrib*^{1} compared with *egr*$^{1/3}$ *scrib*^{1}, for *scrib*^{1} compared with *FRT*, and for *egr*$^{1/3}$ *scrib*^{1} compared with *FRT*.

signalling, we examined whether global removal of *egr* reduced apoptosis in *rok*^{CAT} clones (Fig. 9C). In *rok*^{CAT} clones in a homozygous *egr* mutant background, apoptosis was strongly reduced throughout the EAD, but not eliminated, and the *rok*^{CAT} clones did not overgrow (Fig. 9C compared with 9A,B; quantified in 9D). This was in contrast to the effect of the *egr* mutation on blocking apoptosis in *scrib* mutant tissue, which eliminated apoptotic cells and resulted in overgrowth of the *scrib* mutant clones (Cordero et al., 2010; Igaki et al., 2009) (Fig. 9E). These results suggest that an extrinsic mechanism involving TNF (Egr)-induced JNK activation plays an important role in the increased apoptosis that occurs in *rok*^{CAT} clones. However, because apoptosis was not completely eliminated in *rok*^{CAT} clones in an *egr* mutant background, this suggests that another mechanism also contributes to JNK activation and the increased cell death in *rok*^{CAT} mosaic EADs (see Discussion).

DISCUSSION

In this study, we have dissected the contribution of the RhoGEF2 pathway in Ras-mediated tumorigenesis in *Drosophila* epithelial tissues. We show here that the cooperation of RhoGEF2 with activated Raf phenocopies that observed with Ras^{ACT}. Moreover, our analysis revealed that Rho1, Rok and Myosin II, but not Rac, Dia, Limk or PKN, are important downstream of RhoGEF2 for cooperation with Ras^{ACT} (or Raf^{GOF}). We also demonstrated that the RhoGEF2–Rho1–Rok–Myosin-II pathway contributes to JNK activation in cooperative tumorigenesis with Ras^{ACT} (or Raf^{GOF}). Indeed, activation of Rok or Myosin II alone is sufficient for cooperative tumorigenesis with Ras^{ACT} and induces JNK activity in association with Ras^{ACT}. Cooperative tumorigenesis of RhoGEF2, Rho1 and Rok with Ras^{ACT} is correlated with increased F-actin; however, activation of Myosin II with Ras^{ACT} is not, suggesting that actin-myosin contractility might be an important factor in cooperative tumorigenesis with Ras^{ACT}. Moreover, we show that TNF (Egr)-JNK activation plays an important role in Rok^{CAT}-induced cell death; however, because apoptosis was still observed in an *egr* mutant background, a more direct effect of Rok–Myosin-II on JNK activation might also be involved (see below). These findings are likely to have important implications in the understanding of human Ras-driven cancers.

Contribution of Rho1 effectors to F-actin accumulation in RhoGEF2 clones

The Rho1 effectors Dia, Rok, Limk and PKN have all been shown previously to induce actin polymerisation (Grosshans et al., 2005; Maekawa et al., 1999; Ohashi et al., 2000a; Ohashi et al., 2000b; Vincent and Settleman, 1997). Our results here have revealed that the accumulation of F-actin in RhoGEF2-expressing clones depends on Rho1 and Rok as expected; however, knocking down Limk, Dia or PKN did not significantly reduce F-actin levels in *RhoGEF2* + *Ras*^{ACT}-expressing clones. It is possible that these Rho1 effectors could play more minor roles or act redundantly, such that double or triple knockdowns are required to reduce F-actin levels in RhoGEF2-expressing cells. Interestingly, we found that reducing Myosin II heavy chain levels (using *zip*^{RNAi}) also led to reduced F-actin levels in *RhoGEF2* + *Ras*^{ACT}-expressing clones. This was unexpected given the role of Myosin II in actin-myosin contractility, but not in actin polymerisation. However, expression of activated Myosin II light chain (Sqh^{EE}) did not lead to upregulation of F-actin, suggesting that it is more likely that Myosin II heavy chain depletion might have secondary effects on the regulation of F-actin polymerisation, perhaps due to reduced levels of F-actin–Myosin-II fibres upon the depletion of Myosin II protein, or to feedback mechanisms that affect the activity of actin polymerisation regulators. Nonetheless, the cooperation of Sqh^{EE} with Ras^{ACT} in

tumorigenesis without effects on F-actin suggests that actin-myosin contractility or other events triggered by activated Myosin II light chain are crucial for cooperative tumorigenesis.

The Rho1–Rok–Myosin-II pathway in JNK activation and Ras^{ACT}-mediated tumorigenesis

From data presented here, as well as in our previous study (Brumby et al., 2011), we have shown that Rho1, Rok and Myosin II activity are necessary and sufficient for cooperative tumorigenesis with Ras^{ACT} (Fig. 10). This pathway leads to the activation of JNK (Brumby et al., 2011), which is important for invasion, and the blockage of differentiation and pupation, enabling the tumour to overgrow through an extended larval phase (Brumby et al., 2011; Leong et al., 2009). Blocking JNK activity (using a dominant negative transgene) in RhoGEF2 + Ras^{ACT} tumours results in increased differentiation and pupation (Brumby et al., 2011). In tumorigenesis with Ras^{ACT}, JNK has been shown to be activated by a cell extrinsic mechanism in *scrib* mutant tissue, via TNF (Egr) supplied by the haemocytes (Cordero et al., 2010; Igaki et al., 2009; Lolo et al., 2012; Ohsawa et al., 2011). We have shown that the TNF pathway is partially responsible for the increased apoptosis in Rok^{CAT} EADs; however, unlike *scrib* mutant tissue (Cordero et al., 2010; Igaki et al., 2009), cell death was not completely eliminated in an *egr* mutant background and the clones did not overgrow. Therefore, it is likely that a novel mechanism also exists for JNK activation and/or triggering apoptosis by Rok^{CAT}.

Previous studies have provided evidence that the Rho1–Rok–Myosin-II pathway activates JNK, although the precise mechanism is not clear. One study showed that loss of the cell polarity regulators aPKC, Cdc42 or Par6 results in Rho1–Rok–Myosin-II pathway activation of JNK-dependent apoptosis and compensatory proliferation (Warner et al., 2010). Interestingly, this study showed that JNK activation was independent of Rho1-Rok pathway effects on F-actin polymerisation, because inhibiting Cofilin (by reducing levels of Slingshot, a Cofilin phosphatase, which activates Cofilin) and thereby promoting F-actin stabilisation, did not result in JNK activation or hyperproliferation when apoptosis was blocked. This result is consistent with our finding that activation of Myosin II activity (via *sqh^{EE}* expression) results in cooperative tumorigenesis with *Ras^{ACT}* without upregulation of F-actin. Another study revealed that overexpression of wild-type Rho1 in the anterior-posterior boundary of the developing wing epithelium resulted in JNK-mediated apoptosis (Vidal et al., 2006). Myosin II activity has also been linked to JNK activation in a study of the *Drosophila* non-muscle myosin phosphatase PP1β (Flapwing), which negatively regulates JNK activity through the inhibition of Myosin II activity in the developing wing (Kirchner et al., 2007). Furthermore, a recent study has shown that depletion of the Sds22/PP1 phosphatase can cooperate with Ras^{ACT}, via upregulation of Myosin II activity and JNK activation (Jiang et al., 2011). However, in all of these studies, cell morphology changes occur and might induce recruitment of haemocytes and the activation of JNK via the extrinsic TNF (Egr) pathway. There are, however, examples where JNK is induced without cell morphology changes, such as in response to cellular damage due to irradiation, which is due to a feedback loop involving caspases and p53 (Shlevkov and Morata, 2012), and by oxidative stress, which induces reactive oxygen species (ROS) that activate JNK (Ohsawa et al., 2012; Wang et al., 2003). However, in both these examples, there is evidence suggesting that Egr could also be involved in JNK activation (Kanda et al., 2011; Shlevkov and Morata, 2012). Although we have shown that Rok^{CAT}-induced apoptosis shows a strong dependence on Egr, the fact that there was still some remaining apoptotic cells might suggest that an Egr-independent mechanism is also induced. Whether this mechanism involves p53, Ros or more direct effects of Myosin II on JNK activity remains to be determined. It is possible that activated Myosin II activates JNK directly, because Sqh and Bsk were shown to form a complex *in vivo* in the large-scale proteomics project carried out in *Drosophila* cultured cells (Guruharsha et al., 2011). Furthermore, it is possible that Flapwing or Sds22 phosphatases are inhibited by RhoGEF2-Rho1 signalling and are also involved in Myosin II and JNK activation.

In Ras^{ACT}-driven cooperative tumorigenesis with RhoGEF2 overexpression or Rho1 activation, the activation of JNK is clearly involved in invasion and the block to differentiation and pupation (Brumby et al., 2011). Although we have not yet tested the role of JNK in *rok^{CAT}* or *sqh^{EE}* cooperative tumorigenesis with *Ras^{ACT}*, it most likely plays a similar role. Moreover, JNK might also contribute to cell morphology changes in Ras^{ACT}-driven cooperative tumorigenesis, because blocking JNK activity in wing disc cells depleted for the apico-basal cell polarity regulator Lgl can rescue the cell morphology defects and rescue the overgrowth phenotype (Zhu et al., 2010). JNK might also contribute to the tumour overgrowth: a recent study showed that, in *lgl*-depleted wing disc tissue, JNK can inactivate the Hippo tissue growth control pathway,

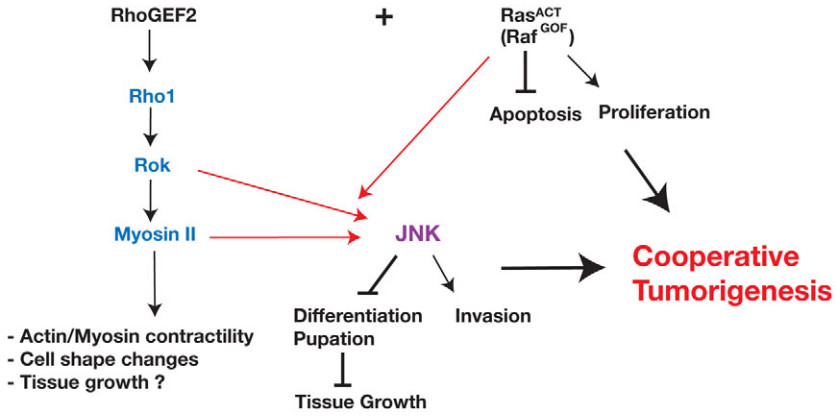

Fig. 10. Model of the RhoGEF2 effector pathway required for cooperation with *Ras^{ACT}* in tumorigenesis. Expression of *Ras^{ACT}* (or *Raf^{GOF}*) alone promotes proliferation and blocks apoptosis, which contributes to the tumour growth. Our epistasis experiments show that RhoGEF2 acts via Rho1–Rok–Myosin-II activity in its cooperation with activated Ras signalling in tumorigenesis. Rho1, Rok and Myosin II are required downstream of RhoGEF2 for JNK activation. Activation of Rok (Rok^{CAT}) or Myosin II activity (Sqh^{EE}) only robustly promotes JNK activation in cooperation with Ras^{ACT}. JNK promotes tumour invasion, and blocks differentiation and pupation, which contributes to the tumour growth during the extended larval stage. Myosin II activity has been documented by others to result in increased F-actin contractility and cell shape changes, but might also contribute to tumour growth in combination with Ras^{ACT}.

thereby promoting tissue overgrowth (Sun and Irvine, 2011). However, in *lgl* mutant clones in the EAD, blocking JNK enhances the clonal overgrowth and leads to loss of polarity and an invasive phenotype (Grzeschik et al., 2010), and blocking JNK in *scrib* mutant EAD clones does not prevent, but rather enhances, the impairment of the Hippo pathway (Doggett et al., 2011). Interestingly, a recent study has revealed that, in $scrib^{-}$ + Ras^{ACT} tumours, JNK activation upregulates expression of an F-actin cross-linking protein, Filamin (Cher), which acts to inhibit the Hippo pathway to promote overgrowth (Külshammer and Uhlirova, 2012). Therefore, although *RhoGEF2-Rho1* + Ras^{ACT}-mediated tumorigenesis requires JNK activation for the block to differentiation and pupation, and to promote invasion, whether JNK can also have a role in cell morphology changes or promoting proliferation via inhibition of the Hippo pathway in these tumours requires further investigation.

Activation of the Rho1–Rok–Myosin-II pathway might also contribute to tumour growth with Ras^{ACT}, independently of JNK (Fig. 10), because our previous analysis has shown that JNK activation alone with Ras^{ACT} does not result in as potent cooperative tumorigenesis as occurs with *RhoGEF2* (or $Rho1^{ACT}$, rok^{CAT} or sqh^{EE}) + Ras^{ACT} (Brumby et al., 2011) (and this study). It is possible that F-actin polymerisation, actin-myosin contractility or cell morphology changes contribute to tumour overgrowth. Recently, increased F-actin polymerisation, due to expression of activated Dia or loss-of-function mutants in the actin capping proteins Cpa and Cpb, was shown to inactivate the Hippo tissue growth control pathway and drive tissue growth (Fernández et al., 2011; Richardson, 2011; Sansores-Garcia et al., 2011). However, as discussed above, RhoGEF2 expression alone did not result in increased cell proliferation in clones, suggesting that a specific form of F-actin is required to regulate the Hippo pathway, which is not generated by the RhoGEF2-Rho1 pathway, or that RhoGEF2 also activates another tissue growth inhibitory pathway. Furthermore, increased F-actin polymerisation seems not to be necessary, because activated Myosin-II regulatory light chain (Sqh^{EE}) induced cooperative tumorigenesis with Ras^{ACT} without affecting F-actin levels.

It is possible that, owing to activation of Myosin II, actin-myosin contractility, cellular tension and cell morphology changes might contribute to tissue growth in *RhoGEF2* + Ras^{ACT} tumours. In mammalian cells, RhoA–Rok–Myosin-II pathway-mediated cell contractility regulates cell proliferation; microinjection of activated forms of RhoA, Rac and Cdc42 in Swiss 3T3 fibroblasts promotes S-phase entry, whereas reducing RhoA, Rac or Cdc42 activity blocked DNA replication (Olson et al., 1995). Actin-myosin contractility can also increase cellular tension, and cellular tension can induce cell proliferation (reviewed by Assoian and Klein, 2008; Mammoto and Ingber, 2009; Yu et al., 2011). Indeed, in cultured monolayers of cells in an elastomeric force sensor array, inhibition of Rok or Myosin II suppressed proliferation, suggesting that contractile force and tension resulting from the RhoA–Rok–Myosin-II pathway regulates cell proliferation (Nelson et al., 2005). More recently, a role for cellular tension in cell proliferation via activation of the Hippo tissue growth control pathway transcriptional co-activator Yap/Taz (homologues of *Drosophila* Yorkie) has been revealed in mammalian cells (Dupont et al., 2011; Wada et al., 2011). The precise mechanism by which this occurs is unclear; however, it has been recently discovered that Scrib can bind to Taz, thereby tethering Taz to the cell cortex (Cordenonsi et al., 2011). Thus, any alteration of cell morphology or cellular tension that leads to mis-localisation of Scrib would release Taz, thereby enabling it to enter the nucleus and upregulate cell survival and proliferation genes. Interestingly, the mechanism was shown in one study to require Rho-GTPase activity (Dupont et al., 2011). Furthermore in a mouse model, activated Rock2 (homologue of *Drosophila* Rok) induced tissue stiffness and activation of the transcription factor β-catenin to promote epidermal hyperplasia (Samuel et al., 2011; Samuel and Olson, 2011). Whether these mechanisms contribute to the tumour growth of RhoGEF2–Rho1–Rok–Myosin-II with activated Ras in *Drosophila* epithelial tissues will require further analysis. Interestingly, a recent study revealed that *Drosophila* Filamin (Cher) binds to Myosin II and is important for activation of Myosin II activity in $scrib^{-}$ + Ras^{ACT} tumours, and also that Myosin II activity is important for tumour overgrowth, via Hippo pathway inactivation, as well as invasion (Külshammer and Uhlirova, 2012). Thus, the cooperation of cell polarity mutants with oncogenic Ras might also require the RhoGEF2–Rho1–Rok–Myosin-II pathway. Indeed, our research here together with this previous study suggests that a positive feedback loop between JNK activation and Myosin II activity might be critical downstream of cell morphology or polarity disruption for cooperative tumorigenesis with oncogenic Ras.

The involvement of RhoGEF2, Rho1, Rok and Myosin II in cooperative tumorigenesis with oncogenic Ras in human cancer

Activation of the Ras signalling pathway occurs in about 30% of all human cancers; however, Ras activation is not sufficient for tumorigenesis because of the induction of cellular senescence (Kern et al., 2011; Serrano et al., 1997). We have identified here that the RhoGEF2–Rho1–Rok–Myosin-II pathway cooperates with oncogenic Ras in *Drosophila* epithelial tissues, raising the question of whether cooperation occurs between these genes in mammalian cancer. There is strong evidence that overexpression of some mammalian RhoGEFs such as Vav1 (Katzav, 2007) and Ect2 (Fields and Justilien, 2010) contribute to human cancers. Furthermore, the mammalian RhoGEF2 homologues PDZ-RhoGEF, p115-RhoGEF and Leukemia associated RhoGEF (LARG) can transform Swiss NIH 3T3 cells (Fukuhara et al., 2001), and *LARG* fused to the mixed lineage leukemia (*MLL*) gene results in acute myeloid leukemia (Kourlas et al., 2000). However, whether Ras is also activated in these cells and contributes to tumorigenesis with the RhoGEFs is not known.

RhoA and Rock (Rok) have been found to be upregulated in many human cancers (reviewed by Karlsson et al., 2009; Narumiya et al., 2009), and upregulation of Rock has been shown to be crucial for RhoA-mediated tumorigenesis (Sahai et al., 1999). Because of this, Rho and Rock have been considered to be good drug targets for cancer therapy (Fritz and Kaina, 2006; Lu et al., 2009; Maruta et al., 2003; Olson, 2008; Rath and Olson, 2012). Whether Ras signalling is also upregulated in cancers in which RhoA or Rock is activated remains to be thoroughly examined. However, *in vitro* studies have revealed that Rho and Rock cooperate with the Ras-Raf pathway in cellular transformation to promote cell proliferation and motility (Coleman et al., 2004; Fleming et al., 2009; Olson et al., 1998; Sahai et al., 1999; Sahai et al., 2001). Furthermore,

activated Rock2 induced epidermal hyperplasia in mice, and after treatment with carcinogens promoted the formation of papillomas and progression to carcinomas (Samuel et al., 2011). The progression of these papillomas to carcinomas is associated with activation of the Ras signalling pathway (Quintanilla et al., 1986), and therefore it is likely that, in this system, the activation of Rock cooperates with activated Ras signalling in tumour progression. Importantly, and consistent with our studies, Samuel et al. showed that the hyperplasia induced by activation of Rock was dependent on Myosin II activity (Samuel et al., 2011). Interestingly, another study reported that actin-myosin contractility can promote K-Ras pathway flux, leading to phosphorylation of Erk; however, this was dependent on Myosin-II light chain kinase, but not Rock (Helfman and Pawlak, 2005). In mammalian cells, activation of Myosin II is not only associated with proliferation (see above), but also cell migration (Clark et al., 2007; Ng et al., 2012). Thus, Myosin II has potentially potent tumorigenic properties that might contribute to Ras-induced mammalian cancer. Whether activation of Myosin II induces JNK to promote these properties in mammalian cells and in human cancer remains to be determined. Thus, further analysis of the mechanism of cooperation between Rock–Myosin-II, JNK activity and oncogenic Ras in mammalian cell models and human cancers is clearly warranted.

MATERIALS AND METHODS

Fly stocks, conditions of culture, overexpression and clonal analysis

Fly stocks used in this study were: *UAS-RhoGEF2* (Mulinari et al., 2008); *UAS-Ras*^{ACT} (Halfar et al., 2001); *UAS-Raf*^{GOF} (Brand and Perrimon, 1994); *UAS-rok*^{CAT} [Bloomington #6669 (Verdier et al., 2006)]; *UAS-sqh*^{EE} [*sqh*^{E20E21} (Wang and Riechmann, 2007)]; *UAS-zip* (Franke et al., 2005); *msn-lacZ* [*msn*^{06946} (Mattila et al., 2005)]; *UAS-Rho*^{RNAi} (#12734 – VDRC); *UAS-Rac1*^{RNAi} (#17411 – VDRC); *UAS-Rac1*^{N17} (Luo et al., 1994); *Rac1, Rac2, mtl* (Hakeda-Suzuki et al., 2002); *UAS-dia*^{RNAi} (#20518 – VDRC); *UAS-PKN*^{RNAi} (#42927 – VDRC); *UAS-Limk*^{RNAi} (#25344 – VDRC); *UAS-rok*^{RNAi} (#3793 – VDRC); *UAS-zip*^{RNAi} (#7819 – VDRC); *UAS-sqh*^{AA} (Jordan and Karess, 1997); the Rho sensor was *UAS-PKN58A-eGFP* (Simões et al., 2006), *scrib*^{1} (Bilder and Perrimon, 2000), and the *egr* homozygous viable alleles, *egr*^{1} and *egr*^{3} (Igaki et al., 2002; Igaki et al., 2009).

The MARCM (mosaic analysis with repressible cell marker) system (Lee and Luo, 2001) with *FRT82B, ey-FLP* and *UAS-GFP* (*eyFLP1, UASmCD8-GFP ;; Tub-GAL4 FRT82B Tub-GAL80/TM6B*) or with *FRT40A, ey-FLP* and *UAS-GFP* (*eyFLP1, UASmCD8-GFP; Tub-GAL80 FRT40A/CyO; Tub-GAL4/TM6B*) were used to induce GFP-positively marked clones. Stocks containing the relevant *UAS*-transgenes and either *FRT82B* or *FRT40A* were generated for clonal analysis using the MARCM system.

Staged lays were carried out by allowing the females in the cross to lay eggs for 8-12 hours before removing the flies. Vials were aged for 5, 7 or 9 days before larvae were collected for dissection. All flies were raised on a standard semolina agar food at 25°C.

Pupation rate

To determine pupation rate, flies were allowed to lay for 12 hours on apple juice agar plates and larvae were left to develop until early third instar at 25°C. Five replicates of 20 larvae of the relevant genotype were placed into fresh food vials. After 9 days AEL, the number of pupae was counted and used to calculate pupation percentage. Data was analysed using GraphPad Prism 5, using a two-tailed *t*-test. Error bars represent standard error of the mean (s.e.m.) and the significance was set at $P<0.05$.

Immunocytochemistry for analysis of *Drosophila* tissues

For analysis of third instar larval EADs, the discs were dissected in PBS, fixed in 4% PFA, washed in PBT (0.1% Triton X-100) and blocked in PBT + 2% normal goat serum. Antibodies used were: mouse Elav [Developmental Studies Hybridoma Bank (DSHB); at 1:20], mouse Mmp1 [DSHB (mouse 5H7B11, 3D8D12, 316B4; at 1/20)], rabbit anti-RhoGEF2 [(Rogers et al., 2004); at 1:200] and mouse β-galactosidase (Rockland; at 1:500). Secondary antibodies were: anti-mouse Alexa-Fluor-647 (Invitrogen; 1:400) or anti-mouse Alexa-Fluor-488 (Invitrogen; 1:400). F-actin was detected with phalloidin-tetramethylrhodamine isothiocyanate (Rhodamine; Sigma; 0.3 mM).

Quantification of F-actin, Mmp1 and Rho1 activity levels

Images of EADs were captured on the Olympus FV Laser Scanning confocal microscope. Multiple EADs were imaged for every genotype. Three clones per EAD were randomly selected and the average pixel intensity in the F-actin, Mmp1 or Rho1 channel was measured using Adobe Photoshop CS3 in two 50×–50 pixel areas, one on either side of the clonal boundary. The average pixel intensity within each clone was normalised using the average pixel intensity outside of that clone. At least three EADs were analysed for each sample. For F-actin measurements, regions of mutant tissue containing cysts, with very high F-actin levels and different morphology compared with the surrounding wild-type tissue, were not used for the measurements. These data for the various samples were then compared using GraphPad Prism 5, using *t*-tests or ANOVA as indicated. Error bars represent s.e.m. and the significance was set at $P<0.05$.

Quantification of β-gal intensity in clones

β-gal intensity of mutant clones was measured by MetaMorph Version 7.7.2.0 after images were captured on the Olympus FV laser scanning confocal microscope. Measurements of β-gal intensity in mutant clones were taken from a ventral or dorsal area of 50×–50 pixels for each EAD section, for at least nine EADs per sample. Only average intensity values over a base line threshold of arbitrary units were recorded. Each measurement was normalised to adjacent wild-type tissue of the same pixel area and expressed as a ratio. The average intensity of β-gal for each sample was compared with others using GraphPad Prism 5, using a two-tailed *t*-test. Error bars represent s.e.m. and the significance was set at $P<0.05$.

TUNEL staining and quantification, and clonal size measurements

TUNEL staining was carried out as described in the manufacturer's protocol (Roche Applied Science). Maximum projections were generated using Fluoview 1.7 Software. Quantification of TUNEL staining was measured by Adobe Photoshop CS5. The number of red pixels was divided by the total area of the EAD as counted in pixels and expressed as a percentage. For determining the clonal size, the area of GFP-marked clones relative to the total area of the

EAD was calculated for each sample, averaged for each genotype and expressed as a percentage. At least five EADs were analysed for each sample. These data for the various samples were then compared using GraphPad Prism 5. Error bars represent s.e.m. and the significance was set at $P<0.05$.

RNA extraction and quantitative real-time PCR

Total RNA was harvested from third instar *Drosophila* larvae by homogenising cells with TRIzol reagent according to the manufacturer's instructions (Invitrogen). cDNA was created from 2 μg total RNA using random primers and M-MLV reverse transcriptase RNase H (Promega), and amplified by PCR in triplicate with SYBR Green® dye detection method (Agilent Technologies) as per the manufacturer's specifications. PCR product detection, using the *Limk* primers listed below, was performed on the ABI PRISM 7700 system (Applied Biosystems), under standard conditions and normalised with a GFP control.

Primers used were: *Limk* forward 5′-TCGGACTTCA-GTCTCAATCAG-3′; *Limk* reverse 5′-GGGATTAAGATCA-CAGCACAC-3′.

ACKNOWLEDGEMENTS

We are grateful to Linda Parsons for critical review of the manuscript, and to all members of the Richardson lab for helpful discussions during the course of this work. We thank Steven Rogers, Udo Hacker, Dan Kiehart, Barry Dickson, the Bloomington Stock Center and the Developmental Studies Hybridoma Bank for fly stocks and antibodies. We acknowledge the Flybase website resource, which greatly facilitated this study.

COMPETING INTERESTS

The authors declare that they do not have any competing or financial interests.

AUTHOR CONTRIBUTIONS

H.E.R. and A.M.B. conceived the study and designed the experiments. P.K. and K.A. carried out all experiments and A.M.B. and H.E.R. assisted with stock generation. P.K., K.A., H.E.R. and A.M.B. interpreted the data. L.W. carried out pixel intensity measurements, comparisons and statistical analysis. H.E.R. and P.K. wrote the paper, K.A. and L.W. contributing to the method descriptions, P.K., K.A., L.W. and H.E.R. prepared the figures, and A.M.B. contributed editorial guidance. All authors read and approved the final manuscript.

FUNDING

This work was supported by the National Health & Medical Research (NHMRC) grants 350369 and 400211, The Oncology Childhood Foundation (OCF), and funds from the Peter MacCallum Cancer Centre (PMCC) to H.E.R. P.K. was supported by an Australian Postgraduate Award, K.A. from the OCF, L.W. from the PMCC and A.M.B. from NHMRC 350396 and 509051 grants, and H.E.R. by a NHMRC Senior Research Fellowship.

SUPPLEMENTARY MATERIAL

Supplementary material for this article is available at
http://dmm.biologists.org/lookup/suppl/doi:10.1242/dmm.010066/-/DC1

REFERENCES

Amano, M., Nakayama, M. and Kaibuchi, K. (2010). Rho-kinase/ROCK: A key regulator of the cytoskeleton and cell polarity. *Cytoskeleton (Hoboken)* **67**, 545-554.

Assoian, R. K. and Klein, E. A. (2008). Growth control by intracellular tension and extracellular stiffness. *Trends Cell Biol.* **18**, 347-352.

Baek, S. H., Kwon, Y.-C., Lee, H. and Choe, K.-M. (2010). Rho-family small GTPases are required for cell polarization and directional sensing in Drosophila wound healing. *Biochem. Biophys. Res. Commun.* **394**, 488-492.

Barrett, K., Leptin, M. and Settleman, J. (1997). The Rho GTPase and a putative RhoGEF mediate a signaling pathway for the cell shape changes in Drosophila gastrulation. *Cell* **91**, 905-915.

Bilder, D. and Perrimon, N. (2000). Localization of apical epithelial determinants by the basolateral PDZ protein Scribble. *Nature* **403**, 676-680.

Brand, A. H. and Perrimon, N. (1994). Raf acts downstream of the EGF receptor to determine dorsoventral polarity during Drosophila oogenesis. *Genes Dev.* **8**, 629-639.

Brumby, A. M. and Richardson, H. E. (2003). scribble mutants cooperate with oncogenic Ras or Notch to cause neoplastic overgrowth in Drosophila. *EMBO J.* **22**, 5769-5779.

Brumby, A. M. and Richardson, H. E. (2005). Using Drosophila melanogaster to map human cancer pathways. *Nat. Rev. Cancer* **5**, 626-639.

Brumby, A. M., Goulding, K. R., Schlosser, T., Loi, S., Galea, R., Khoo, P., Bolden, J. E., Aigaki, T., Humbert, P. O. and Richardson, H. E. (2011). Identification of novel Ras-cooperating oncogenes in Drosophila melanogaster: a RhoGEF/Rho-family/JNK pathway is a central driver of tumorigenesis. *Genetics* **188**, 105-125.

Clark, K., Langeslag, M., Figdor, C. G. and van Leeuwen, F. N. (2007). Myosin II and mechanotransduction: a balancing act. *Trends Cell Biol.* **17**, 178-186.

Coleman, M. L., Marshall, C. J. and Olson, M. F. (2004). RAS and RHO GTPases in G1-phase cell-cycle regulation. *Nat. Rev. Mol. Cell Biol.* **5**, 355-366.

Cordenonsi, M., Zanconato, F., Azzolin, L., Forcato, M., Rosato, A., Frasson, C., Inui, M., Montagner, M., Parenti, A. R., Poletti, A. et al. (2011). The Hippo transducer TAZ confers cancer stem cell-related traits on breast cancer cells. *Cell* **147**, 759-772.

Cordero, J. B., Macagno, J. P., Stefanatos, R. K., Strathdee, K. E., Cagan, R. L. and Vidal, M. (2010). Oncogenic Ras diverts a host TNF tumor suppressor activity into tumor promoter. *Dev. Cell* **18**, 999-1011.

Dawes-Hoang, R. E., Parmar, K. M., Christiansen, A. E., Phelps, C. B., Brand, A. H. and Wieschaus, E. F. (2005). folded gastrulation, cell shape change and the control of myosin localization. *Development* **132**, 4165-4178.

Derivery, E. and Gautreau, A. (2010). Generation of branched actin networks: assembly and regulation of the N-WASP and WAVE molecular machines. *Bioessays* **32**, 119-131.

Doggett, K., Grusche, F. A., Richardson, H. E. and Brumby, A. M. (2011). Loss of the Drosophila cell polarity regulator Scribbled promotes epithelial tissue overgrowth and cooperation with oncogenic Ras-Raf through impaired Hippo pathway signaling. *BMC Dev. Biol.* **11**, 57.

Dupont, S., Morsut, L., Aragona, M., Enzo, E., Giulitti, S., Cordenonsi, M., Zanconato, F., Le Digabel, J., Forcato, M., Bicciato, S. et al. (2011). Role of YAP/TAZ in mechanotransduction. *Nature* **474**, 179-183.

Faulstich, H., Trischmann, H. and Mayer, D. (1983). Preparation of tetramethylrhodaminyl-phalloidin and uptake of the toxin into short-term cultured hepatocytes by endocytosis. *Exp. Cell Res.* **144**, 73-82.

Fernández, B. G., Gaspar, P., Brás-Pereira, C., Jezowska, B., Rebelo, S. R. and Janody, F. (2011). Actin-Capping Protein and the Hippo pathway regulate F-actin and tissue growth in Drosophila. *Development* **138**, 2337-2346.

Fields, A. P. and Justilien, V. (2010). The guanine nucleotide exchange factor (GEF) Ect2 is an oncogene in human cancer. *Adv. Enzyme Regul.* **50**, 190-200.

Fleming, Y. M., Ferguson, G. J., Spender, L. C., Larsson, J., Karlsson, S., Ozanne, B. W., Grosse, R. and Inman, G. J. (2009). TGF-beta-mediated activation of RhoA signalling is required for efficient (V12)HaRas and (V600E)BRAF transformation. *Oncogene* **28**, 983-993.

Franke, J. D., Montague, R. A. and Kiehart, D. P. (2005). Nonmuscle myosin II generates forces that transmit tension and drive contraction in multiple tissues during dorsal closure. *Curr. Biol.* **15**, 2208-2221.

Fritz, G. and Kaina, B. (2006). Rho GTPases: promising cellular targets for novel anticancer drugs. *Curr. Cancer Drug Targets* **6**, 1-14.

Fukuhara, S., Chikumi, H. and Gutkind, J. S. (2001). RGS-containing RhoGEFs: the missing link between transforming G proteins and Rho? *Oncogene* **20**, 1661-1668.

Glise, B. and Noselli, S. (1997). Coupling of Jun amino-terminal kinase and Decapentaplegic signaling pathways in Drosophila morphogenesis. *Genes Dev.* **11**, 1738-1747.

Grosshans, J., Wenzl, C., Herz, H.-M., Bartoszewski, S., Schnorrer, F., Vogt, N., Schwarz, H. and Müller, H.-A. (2005). RhoGEF2 and the formin Dia control the formation of the furrow canal by directed actin assembly during Drosophila cellularisation. *Development* **132**, 1009-1020.

Grzeschik, N. A., Parsons, L. M. and Richardson, H. E. (2010). Lgl, the SWH pathway and tumorigenesis: It's a matter of context and competition! *Cell Cycle* **9**, 3202-3212.

Guruharsha, K. G., Rual, J. F., Zhai, B., Mintseris, J., Vaidya, P., Vaidya, N., Beekman, C., Wong, C., Rhee, D. Y., Cenaj, O. et al. (2011). A protein complex network of Drosophila melanogaster. *Cell* **147**, 690-703.

Häcker, U. and Perrimon, N. (1998). DRhoGEF2 encodes a member of the Dbl family of oncogenes and controls cell shape changes during gastrulation in Drosophila. *Genes Dev.* **12**, 274-284.

Hacker, B. M., Tomlinson, J. E., Wayman, G. A., Sultana, R., Chan, G., Villacres, E., Disteche, C. and Storm, D. R. (1998). Cloning, chromosomal mapping, and regulatory properties of the human type 9 adenylyl cyclase (ADCY9). *Genomics* **50**, 97-104.

Hakeda-Suzuki, S., Ng, J., Tzu, J., Dietzl, G., Sun, Y., Harms, M., Nardine, T., Luo, L. and Dickson, B. J. (2002). Rac function and regulation during Drosophila development. *Nature* **416**, 438-442.

Halfar, K., Rommel, C., Stocker, H. and Hafen, E. (2001). Ras controls growth, survival and differentiation in the Drosophila eye by different thresholds of MAP kinase activity. *Development* **128**, 1687-1696.

Halsell, S. R., Chu, B. I. and Kiehart, D. P. (2000). Genetic analysis demonstrates a direct link between rho signaling and nonmuscle myosin function during Drosophila morphogenesis. *Genetics* **156**, 469.
Hanahan, D. and Weinberg, R. A. (2000). The hallmarks of cancer. *Cell* **100**, 57-70.
Hanahan, D. and Weinberg, R. A. (2011). Hallmarks of cancer: the next generation. *Cell* **144**, 646-674.
Helfman, D. M. and Pawlak, G. (2005). Myosin light chain kinase and acto-myosin contractility modulate activation of the ERK cascade downstream of oncogenic Ras. *J. Cell. Biochem.* **95**, 1069-1080.
Hou, X. S., Goldstein, E. S. and Perrimon, N. (1997). Drosophila Jun relays the Jun amino-terminal kinase signal transduction pathway to the Decapentaplegic signal transduction pathway in regulating epithelial cell sheet movement. *Genes Dev.* **11**, 1728-1737.
Igaki, T., Kanda, H., Yamamoto-Goto, Y., Kanuka, H., Kuranaga, E., Aigaki, T. and Miura, M. (2002). Eiger, a TNF superfamily ligand that triggers the Drosophila JNK pathway. *EMBO J.* **21**, 3009-3018.
Igaki, T., Pastor-Pareja, J. C., Aonuma, H., Miura, M. and Xu, T. (2009). Intrinsic tumor suppression and epithelial maintenance by endocytic activation of Eiger/TNF signaling in Drosophila. *Dev. Cell* **16**, 458-465.
Jaffe, A. B. and Hall, A. (2005). Rho GTPases: biochemistry and biology. *Annu. Rev. Cell Dev. Biol.* **21**, 247-269.
Jiang, Y., Scott, K. L., Kwak, S. J., Chen, R. and Mardon, G. (2011). Sds22/PP1 links epithelial integrity and tumor suppression via regulation of myosin II and JNK signaling. *Oncogene* **30**, 3248-3260.
Johndrow, J. E., Magie, C. R. and Parkhurst, S. M. (2004). Rho GTPase function in flies: insights from a developmental and organismal perspective. *Biochem. Cell Biol.* **82**, 643-657.
Jordan, P. and Karess, R. (1997). Myosin light chain-activating phosphorylation sites are required for oogenesis in Drosophila. *J. Cell Biol.* **139**, 1805-1819.
Kanda, H., Igaki, T., Okano, H. and Miura, M. (2011). Conserved metabolic energy production pathways govern Eiger/TNF-induced nonapoptotic cell death. *Proc. Natl. Acad. Sci. USA* **108**, 18977-18982.
Karim, F. D. and Rubin, G. M. (1998). Ectopic expression of activated Ras1 induces hyperplastic growth and increased cell death in Drosophila imaginal tissues. *Development* **125**, 1-9.
Karlsson, R., Pedersen, E. D., Wang, Z. and Brakebusch, C. (2009). Rho GTPase function in tumorigenesis. *Biochim. Biophys. Acta* **1796**, 91-98.
Katzav, S. (2007). Flesh and blood: the story of Vav1, a gene that signals in hematopoietic cells but can be transforming in human malignancies. *Cancer Lett.* **255**, 241-254.
Kern, F., Niault, T. and Baccarini, M. (2011). Ras and Raf pathways in epidermis development and carcinogenesis. *Br. J. Cancer* **104**, 229-234.
Kirchner, J., Gross, S., Bennett, D. and Alphey, L. (2007). The nonmuscle myosin phosphatase PP1beta (flapwing) negatively regulates Jun N-terminal kinase in wing imaginal discs of Drosophila. *Genetics* **175**, 1741-1749.
Kourlas, P. J., Strout, M. P., Becknell, B., Veronese, M. L., Croce, C. M., Theil, K. S., Krahe, R., Ruutu, T., Knuutila, S., Bloomfield, C. D. et al. (2000). Identification of a gene at 11q23 encoding a guanine nucleotide exchange factor: evidence for its fusion with MLL in acute myeloid leukemia. *Proc. Natl. Acad. Sci. USA* **97**, 2145-2150.
Külshammer, E. and Uhlirova, M. (2012). The actin cross-linker Filamin/Cheerio mediates tumor malignancy downstream of JNK signaling. *J. Cell Sci.* [Epub ahead of print] doi: 10.1242/jcs.114462.
Kwon, Y.-C., Baek, S. H., Lee, H. and Choe, K.-M. (2010). Nonmuscle myosin II localization is regulated by JNK during Drosophila larval wound healing. *Biochem. Biophys. Res. Commun.* **393**, 656-661.
Lee, T. and Luo, L. (2001). Mosaic analysis with a repressible cell marker (MARCM) for Drosophila neural development. *Trends Neurosci.* **24**, 251-254.
Leong, G. R., Goulding, K. R., Amin, N., Richardson, H. E. and Brumby, A. M. (2009). Scribble mutants promote aPKC and JNK-dependent epithelial neoplasia independently of Crumbs. *BMC Biol.* **7**, 62.
Leptin, M. (1999). Gastrulation in Drosophila: the logic and the cellular mechanisms. *EMBO J.* **18**, 3187-3192.
Lolo, F. N., Casas-Tintó, S. and Moreno, E. (2012). Cell competition time line: winners kill losers, which are extruded and engulfed by hemocytes. *Cell Rep.* **2**, 526-539.
Lu, Y. and Settleman, J. (1999). The Drosophila Pkn protein kinase is a Rho/Rac effector target required for dorsal closure during embryogenesis. *Genes Dev.* **13**, 1168-1180.
Lu, Q., Longo, F. M., Zhou, H., Massa, S. M. and Chen, Y. H. (2009). Signaling through Rho GTPase pathway as viable drug target. *Curr. Med. Chem.* **16**, 1355-1365.
Luo, L., Liao, Y. J., Jan, L. Y. and Jan, Y. N. (1994). Distinct morphogenetic functions of similar small GTPases: Drosophila Drac1 is involved in axonal outgrowth and myoblast fusion. *Genes Dev.* **8**, 1787-1802.
Maekawa, M., Ishizaki, T., Boku, S., Watanabe, N., Fujita, A., Iwamatsu, A., Obinata, T., Ohashi, K., Mizuno, K. and Narumiya, S. (1999). Signaling from Rho to the actin cytoskeleton through protein kinases ROCK and LIM-kinase. *Science* **285**, 895-898.
Mammoto, A. and Ingber, D. E. (2009). Cytoskeletal control of growth and cell fate switching. *Curr. Opin. Cell Biol.* **21**, 864-870.
Maruta, H., Nheu, T. V., He, H. and Hirokawa, Y. (2003). Rho family-associated kinases PAK1 and rock. *Prog. Cell Cycle Res.* **5**, 203-210.
Massarwa, R., Schejter, E. D. and Shilo, B.-Z. (2009). Apical secretion in epithelial tubes of the Drosophila embryo is directed by the Formin-family protein Diaphanous. *Dev. Cell* **16**, 877-888.
Mattila, J., Omelyanchuk, L., Kyttälä, S., Turunen, H. and Nokkala, S. (2005). Role of Jun N-terminal Kinase (JNK) signaling in the wound healing and regeneration of a Drosophila melanogaster wing imaginal disc. *Int. J. Dev. Biol.* **49**, 391-399.
Mulinari, S., Barmchi, M. P. and Häcker, U. (2008). DRhoGEF2 and diaphanous regulate contractile force during segmental groove morphogenesis in the Drosophila embryo. *Mol. Biol. Cell* **19**, 1883-1892.
Narumiya, S., Tanji, M. and Ishizaki, T. (2009). Rho signaling, ROCK and mDia1, in transformation, metastasis and invasion. *Cancer Metastasis Rev.* **28**, 65-76.
Neisch, A. L., Speck, O., Stronach, B. and Fehon, R. G. (2010). Rho1 regulates apoptosis via activation of the JNK signaling pathway at the plasma membrane. *J. Cell Biol.* **189**, 311-323.
Nelson, C. M., Jean, R. P., Tan, J. L., Liu, W. F., Sniadecki, N. J., Spector, A. A. and Chen, C. S. (2005). Emergent patterns of growth controlled by multicellular form and mechanics. *Proc. Natl. Acad. Sci. USA* **102**, 11594-11599.
Ng, M. R., Besser, A., Danuser, G. and Brugge, J. S. (2012). Substrate stiffness regulates cadherin-dependent collective migration through myosin-II contractility. *J. Cell Biol.* **199**, 545-563.
Ohashi, K., Hosoya, T., Takahashi, K., Hing, H. and Mizuno, K. (2000a). A Drosophila homolog of LIM-kinase phosphorylates cofilin and induces actin cytoskeletal reorganization. *Biochem. Biophys. Res. Commun.* **276**, 1178-1185.
Ohashi, K., Nagata, K., Maekawa, M., Ishizaki, T., Narumiya, S. and Mizuno, K. (2000b). Rho-associated kinase ROCK activates LIM-kinase 1 by phosphorylation at threonine 508 within the activation loop. *J. Biol. Chem.* **275**, 3577-3582.
Ohsawa, S., Sugimura, K., Takino, K., Xu, T., Miyawaki, A. and Igaki, T. (2011). Elimination of oncogenic neighbors by JNK-mediated engulfment in Drosophila. *Dev. Cell* **20**, 315-328.
Ohsawa, S., Sato, Y., Enomoto, M., Nakamura, M., Betsumiya, A. and Igaki, T. (2012). Mitochondrial defect drives non-autonomous tumour progression through Hippo signalling in Drosophila. *Nature* **490**, 547-551.
Olson, M. F. (2008). Applications for ROCK kinase inhibition. *Curr. Opin. Cell Biol.* **20**, 242-248.
Olson, M. F., Ashworth, A. and Hall, A. (1995). An essential role for Rho, Rac, and Cdc42 GTPases in cell cycle progression through G1. *Science* **269**, 1270-1272.
Olson, M. F., Paterson, H. F. and Marshall, C. J. (1998). Signals from Ras and Rho GTPases interact to regulate expression of p21Waf1/Cip1. *Nature* **394**, 295-299.
Pagliarini, R. A. and Xu, T. (2003). A genetic screen in Drosophila for metastatic behavior. *Science* **302**, 1227-1231.
Perrimon, N., Lanjuin, A., Arnold, C. and Noll, E. (1996). Zygotic lethal mutations with maternal effect phenotypes in Drosophila melanogaster. II. Loci on the second and third chromosomes identified by P-element-induced mutations. *Genetics* **144**, 1681-1692.
Quintanilla, M., Brown, K., Ramsden, M. and Balmain, A. (1986). Carcinogen-specific mutation and amplification of Ha-ras during mouse skin carcinogenesis. *Nature* **322**, 78-80.
Rath, N. and Olson, M. F. (2012). Rho-associated kinases in tumorigenesis: re-considering ROCK inhibition for cancer therapy. *EMBO Rep.* **13**, 900-908.
Richardson, H. E. (2011). Actin up for Hippo. *EMBO J.* **30**, 2307-2309.
Robinow, S. and White, K. (1991). Characterization and spatial distribution of the ELAV protein during Drosophila melanogaster development. *J. Neurobiol.* **22**, 443-461.
Rogers, S. L., Wiedemann, U., Häcker, U., Turck, C. and Vale, R. D. (2004). Drosophila RhoGEF2 associates with microtubule plus ends in an EB1-dependent manner. *Curr. Biol.* **14**, 1827-1833.
Rossman, K. L., Der, C. J. and Sondek, J. (2005). GEF means go: turning on RHO GTPases with guanine nucleotide-exchange factors. *Nat. Rev. Mol. Cell Biol.* **6**, 167-180.
Sahai, E., Ishizaki, T., Narumiya, S. and Treisman, R. (1999). Transformation mediated by RhoA requires activity of ROCK kinases. *Curr. Biol.* **9**, 136-145.
Sahai, E., Olson, M. F. and Marshall, C. J. (2001). Cross-talk between Ras and Rho signalling pathways in transformation favours proliferation and increased motility. *EMBO J.* **20**, 755-766.
Samuel, M. S. and Olson, M. F. (2011). Actomyosin contractililty: force power drives tumor growth. *Cell Cycle* **10**, 3409-3410.
Samuel, M. S., Lopez, J. I., McGhee, E. J., Croft, D. R., Strachan, D., Timpson, P., Munro, J., Schröder, E., Zhou, J., Brunton, V. G. et al. (2011). Actomyosin-

mediated cellular tension drives increased tissue stiffness and β-catenin activation to induce epidermal hyperplasia and tumor growth. *Cancer Cell* **19**, 776-791.

Sansores-Garcia, L., Bossuyt, W., Wada, K., Yonemura, S., Tao, C., Sasaki, H. and Halder, G. (2011). Modulating F-actin organization induces organ growth by affecting the Hippo pathway. *EMBO J.* **30**, 2325-2335.

Serrano, M., Lin, A. W., McCurrach, M. E., Beach, D. and Lowe, S. W. (1997). Oncogenic ras provokes premature cell senescence associated with accumulation of p53 and p16INK4a. *Cell* **88**, 593-602.

Settleman, J. (2001). Rac 'n Rho: the music that shapes a developing embryo. *Dev. Cell* **1**, 321-331.

Shlevkov, E. and Morata, G. (2012). A dp53/JNK-dependant feedback amplification loop is essential for the apoptotic response to stress in Drosophila. *Cell Death Differ.* **19**, 451-460.

Simões, S., Denholm, B., Azevedo, D., Sotillos, S., Martin, P., Skaer, H., Hombría, J. C.-G. and Jacinto, A. (2006). Compartmentalisation of Rho regulators directs cell invagination during tissue morphogenesis. *Development* **133**, 4257-4267.

Sun, G. and Irvine, K. D. (2011). Regulation of Hippo signaling by Jun kinase signaling during compensatory cell proliferation and regeneration, and in neoplastic tumors. *Dev. Biol.* **350**, 139-151.

Szczepanowska, J. (2009). Involvement of Rac/Cdc42/PAK pathway in cytoskeletal rearrangements. *Acta Biochim. Pol.* **56**, 225-234.

Uhlirova, M. and Bohmann, D. (2006). JNK- and Fos-regulated Mmp1 expression cooperates with Ras to induce invasive tumors in Drosophila. *EMBO J.* **25**, 5294-5304.

van Impel, A., Schumacher, S., Draga, M., Herz, H.-M., Grosshans, J. and Müller, H. A. J. (2009). Regulation of the Rac GTPase pathway by the multifunctional Rho GEF Pebble is essential for mesoderm migration in the Drosophila gastrula. *Development* **136**, 813-822.

Verdier, V., Guang-Chao-Chen, and Settleman, J. (2006). Rho-kinase regulates tissue morphogenesis via non-muscle myosin and LIM-kinase during Drosophila development. *BMC Dev. Biol.* **6**, 38.

Vidal, M., Larson, D. E. and Cagan, R. L. (2006). Csk-deficient boundary cells are eliminated from normal Drosophila epithelia by exclusion, migration, and apoptosis. *Dev. Cell* **10**, 33-44.

Vincent, S. and Settleman, J. (1997). The PRK2 kinase is a potential effector target of both Rho and Rac GTPases and regulates actin cytoskeletal organization. *Mol. Cell. Biol.* **17**, 2247-2256.

Vogelstein, B. and Kinzler, K. W. (1993). The multistep nature of cancer. *Trends Genet.* **9**, 138-141.

Wada, K., Itoga, K., Okano, T., Yonemura, S. and Sasaki, H. (2011). Hippo pathway regulation by cell morphology and stress fibers. *Development* **138**, 3907-3914.

Wang, Y. and Riechmann, V. (2007). The role of the actomyosin cytoskeleton in coordination of tissue growth during Drosophila oogenesis. *Curr. Biol.* **17**, 1349-1355.

Wang, M. C., Bohmann, D. and Jasper, H. (2003). JNK signaling confers tolerance to oxidative stress and extends lifespan in Drosophila. *Dev. Cell* **5**, 811-816.

Warner, S. J. and Longmore, G. D. (2009). Distinct functions for Rho1 in maintaining adherens junctions and apical tension in remodeling epithelia. *J. Cell Biol.* **185**, 1111-1125.

Warner, S. J., Yashiro, H. and Longmore, G. D. (2010). The Cdc42/Par6/aPKC polarity complex regulates poptosis-induced compensatory proliferation in epithelia. *Curr. Biol.* **20**, 677-686.

Widmann, T. J. and Dahmann, C. (2009). Dpp signaling promotes the cuboidal-to-columnar shape transition of Drosophila wing disc epithelia by regulating Rho1. *J. Cell Sci.* **122**, 1362-1373.

Winter, C. G., Wang, B., Ballew, A., Royou, A., Karess, R., Axelrod, J. D. and Luo, L. (2001). Drosophila Rho-associated kinase (Drok) links Frizzled-mediated planar cell polarity signaling to the actin cytoskeleton. *Cell* **105**, 81-91.

Woolner, S., Jacinto, A. and Martin, P. (2005). The small GTPase Rac plays multiple roles in epithelial sheet fusion – dynamic studies of Drosophila dorsal closure. *Dev. Biol.* **282**, 163-173.

Xu, N., Keung, B. and Myat, M. M. (2008). Rho GTPase controls invagination and cohesive migration of the Drosophila salivary gland through Crumbs and Rho-kinase. *Dev. Biol.* **321**, 88-100.

Yan, J., Lu, Q., Fang, X. and Adler, P. N. (2009). Rho1 has multiple functions in Drosophila wing planar polarity. *Dev. Biol.* **333**, 186-199.

Young, P. E., Richman, A. M., Ketchum, A. S. and Kiehart, D. P. (1993). Morphogenesis in Drosophila requires nonmuscle myosin heavy chain function. *Genes Dev.* **7**, 29-41.

Yu, H., Mouw, J. K. and Weaver, V. M. (2011). Forcing form and function: biomechanical regulation of tumor evolution. *Trends Cell Biol.* **21**, 47-56.

Zhu, M., Xin, T., Weng, S., Gao, Y., Zhang, Y., Li, Q. and Li, M. (2010). Activation of JNK signaling links lgl mutations to disruption of the cell polarity and epithelial organization in Drosophila imaginal discs. *Cell Res.* **20**, 242-245.